

*Supporting Materials*

# Highly Active CO<sub>2</sub> Fixation into Cyclic Carbonates Catalyzed by Tetranuclear Aluminum Benzodiimidazole-Diylidene Adducts

Ángela Mesías-Salazar <sup>1</sup>, Yersica Ríos Yepes <sup>1</sup>, Javier Martínez <sup>2,\*</sup> and René S. Rojas <sup>1,\*</sup>

<sup>1</sup> Laboratorio de Química Inorgánica, Facultad de Química y Farmacia, Pontificia Universidad Católica de Chile, Casilla 306, Santiago 22 6094411, Chile; admesias@uc.cl (A.M.-S.); yrios1@uc.cl (Y.R.Y.)

<sup>2</sup> Instituto de Ciencias Químicas, Facultad de Ciencias, Isla Teja, Universidad Austral de Chile, 5090000 Valdivia, Chile

\* Correspondence: javier.martinez@uach.cl (J.M.); rrojasg@uc.cl (R.S.R); Tel.: 56-2-2354-7557 (R.S.R)

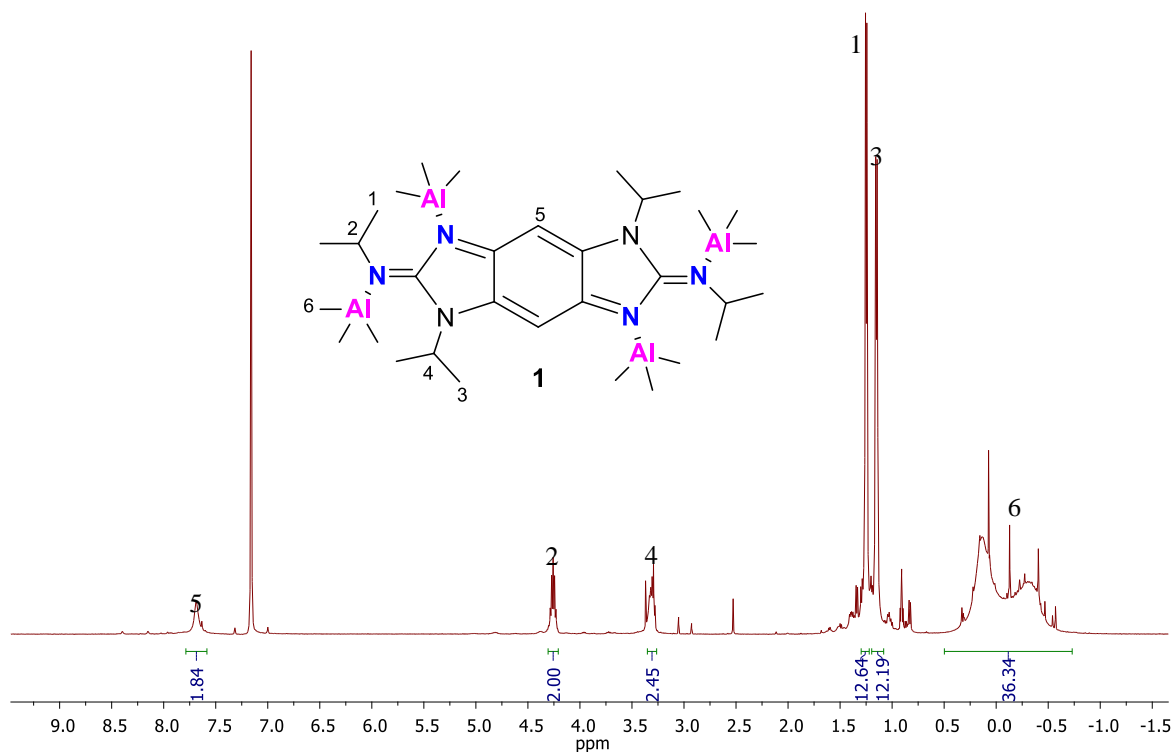


**Figure S1.**  $^1\text{H}$  NMR spectrum for alkyl aluminum adduct **1** in  $\text{C}_6\text{D}_6$ .

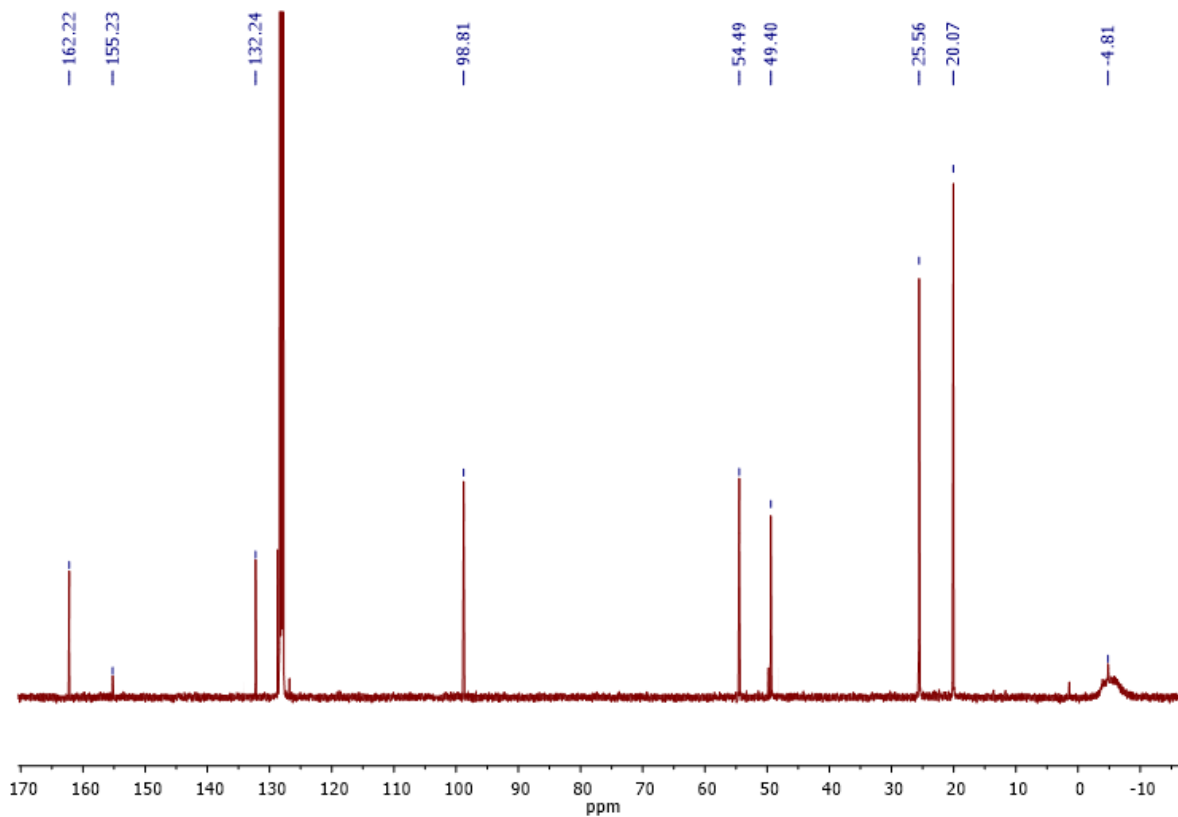


**Figure S2.**  $^{13}\text{C}\{^1\text{H}\}$  NMR spectrum for alkyl aluminum adduct **1** in  $\text{C}_6\text{D}_6$ .

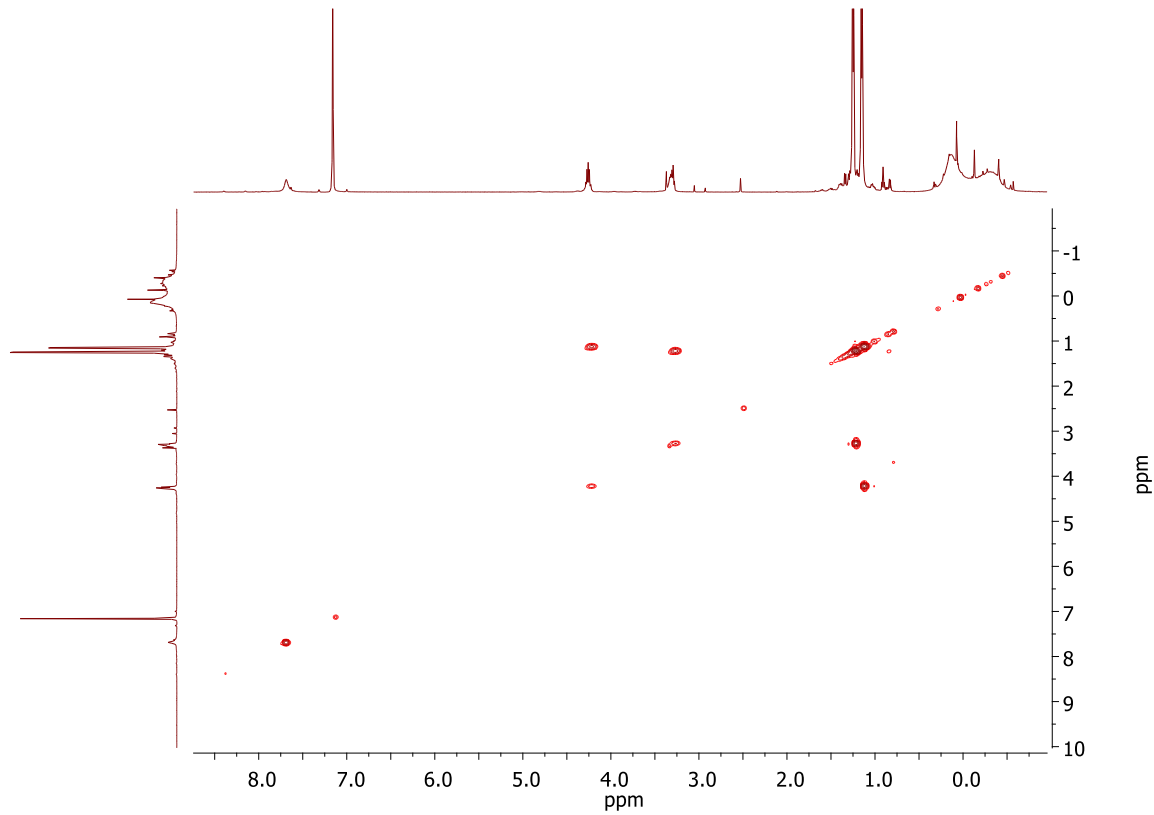


**Figure S3.**  $^1\text{H}$ - $^1\text{H}$  COSY NMR spectrum for alkyl aluminum adduct **1** in  $\text{C}_6\text{D}_6$ .

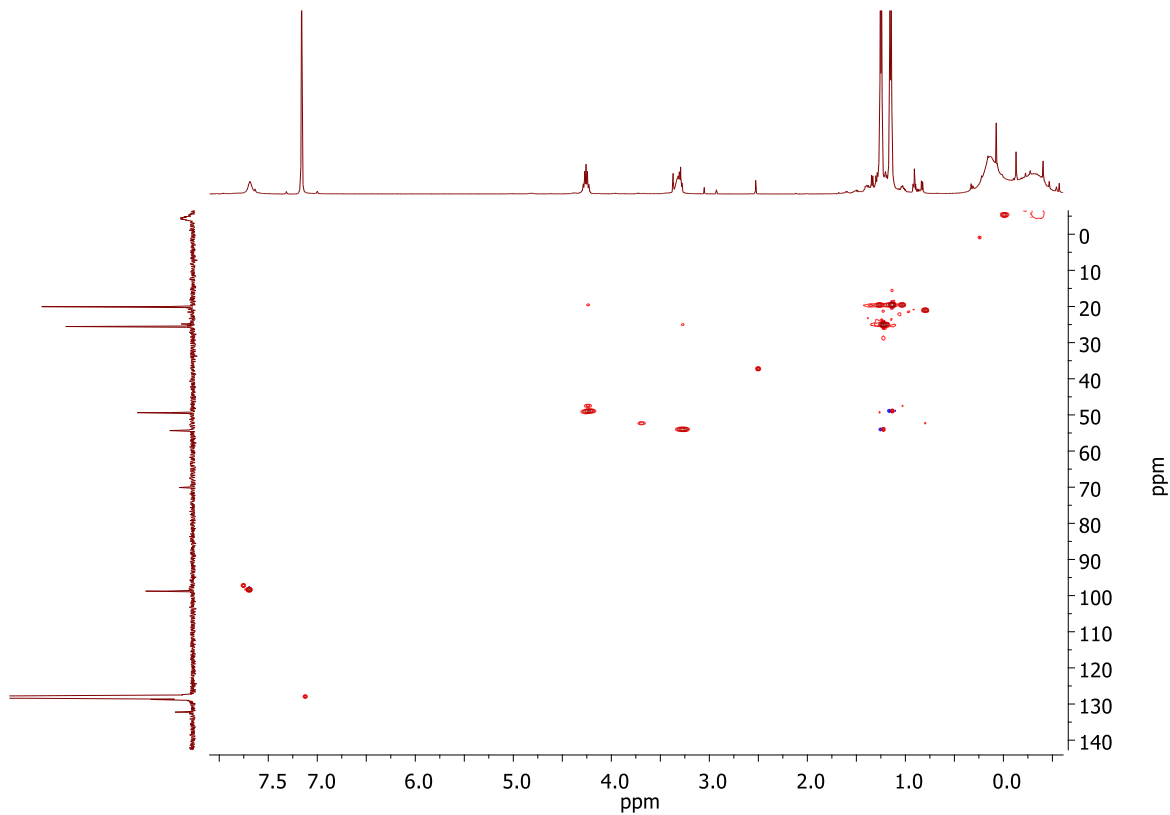


**Figure S4.**  $^{13}\text{C}\{\text{H}\}$ -HMQC NMR spectrum for alkyl aluminum adduct **1** in  $\text{C}_6\text{D}_6$ .

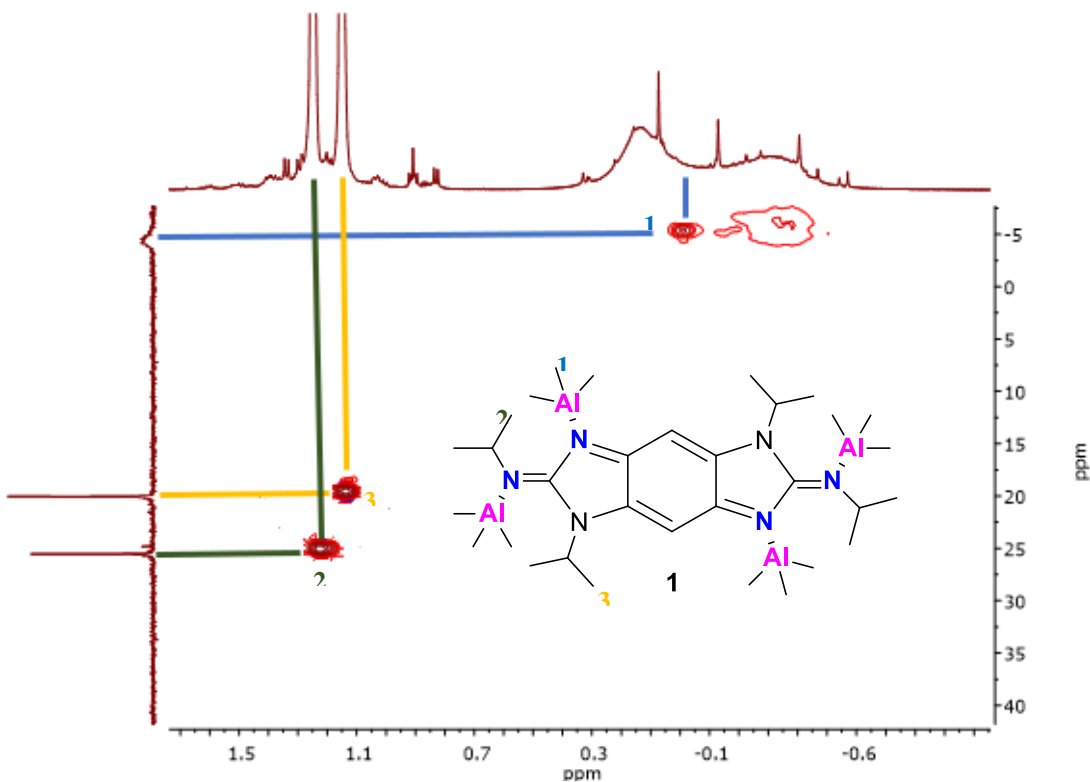


**Figure S5.**  $^{13}\text{C}\{^1\text{H}\}$ -HMQC NMR spectrum for alkyl aluminum adduct **1** in  $\text{C}_6\text{D}_6$  (range (-1.1)-1.7 ppm in  $^1\text{H}$ -NMR and (-7.5)-42.0 ppm in  $^{13}\text{C}$ -NMR).

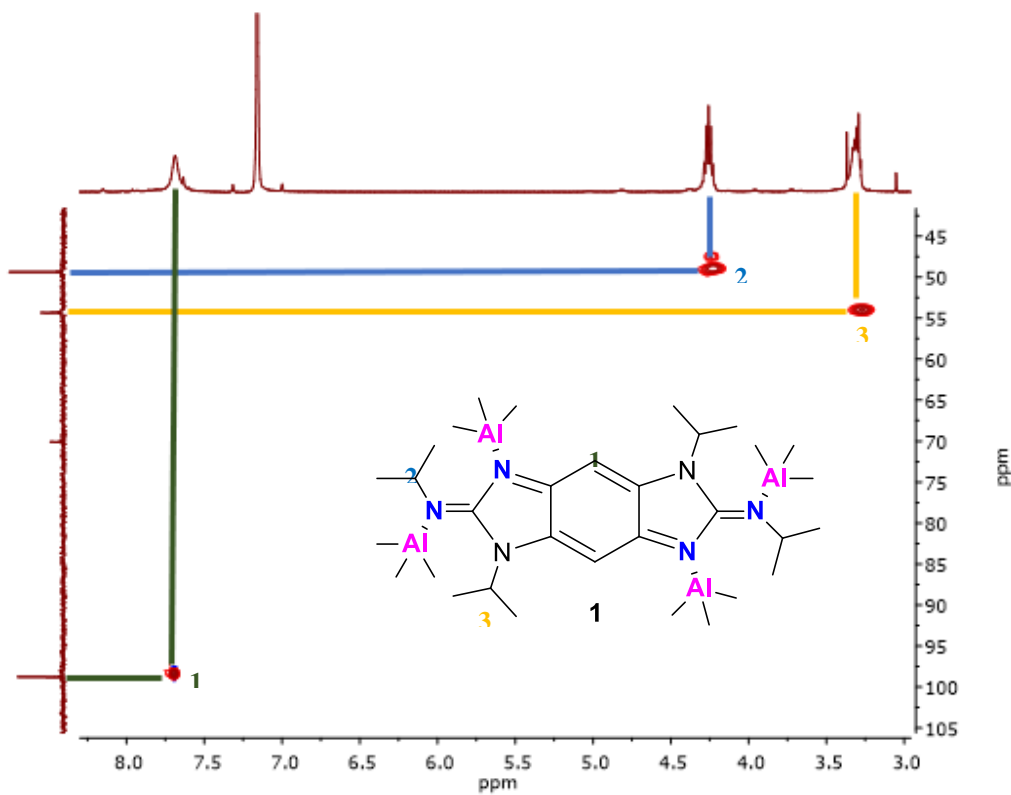


**Figure S6.**  $^{13}\text{C}\{^1\text{H}\}$ -HMQC NMR spectrum for alkyl aluminum adduct **1** in  $\text{C}_6\text{D}_6$  (range 3.0-8.2 ppm in  $^1\text{H}$ -NMR and 42.0-105.0 ppm in  $^{13}\text{C}$ -NMR).

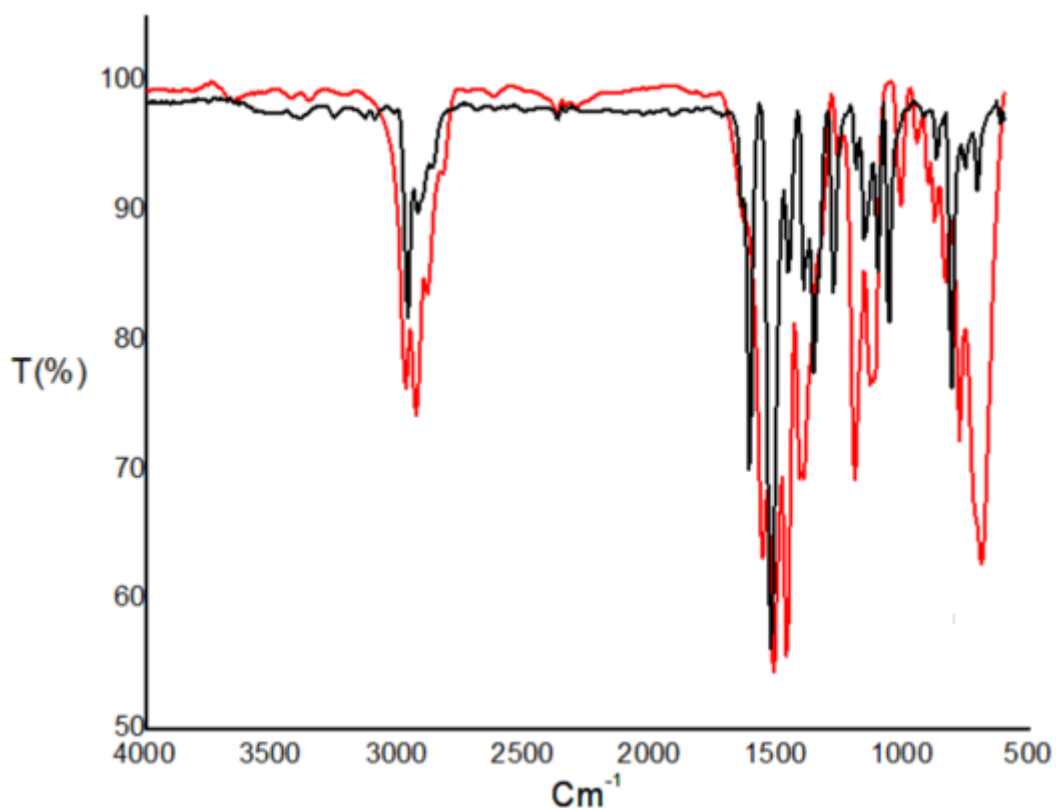
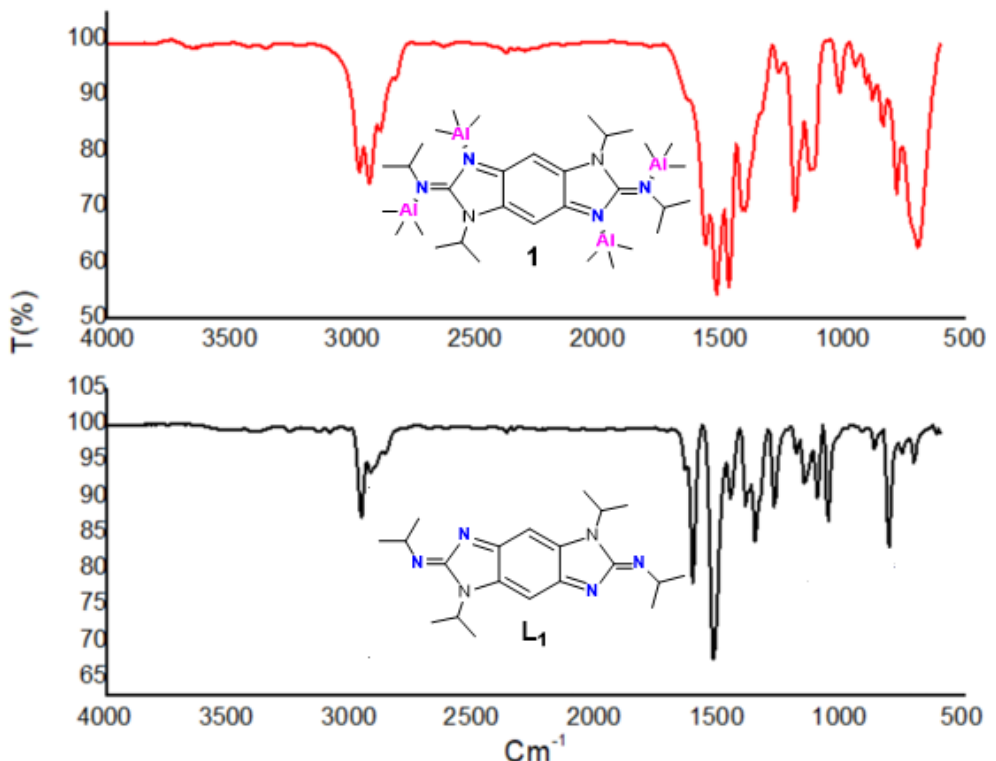


**Figure S7.** FT-IR spectrum for alkyl aluminum adduct **1** (red) versus benzodiimidazole-diylidene ligand **L1** (black).

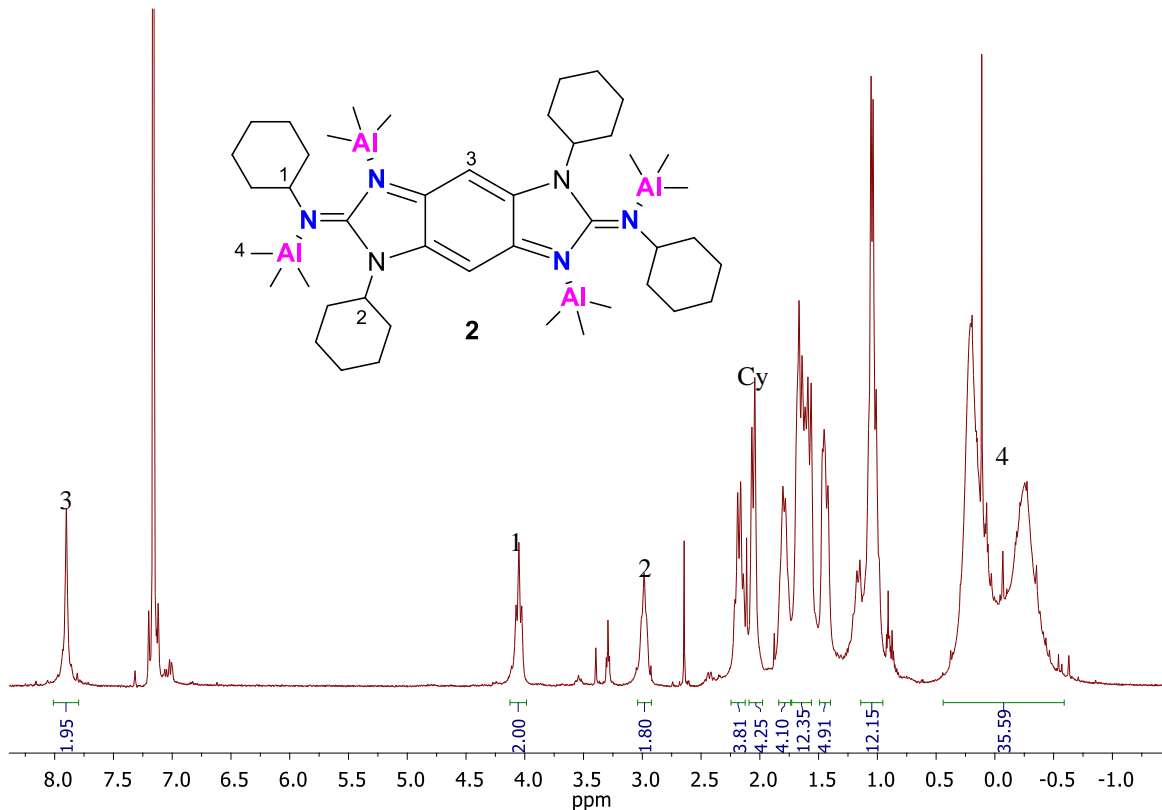


**Figure S8.**  $^1\text{H}$  NMR spectrum for alkyl aluminum adduct **2** in  $\text{C}_6\text{D}_6$ .

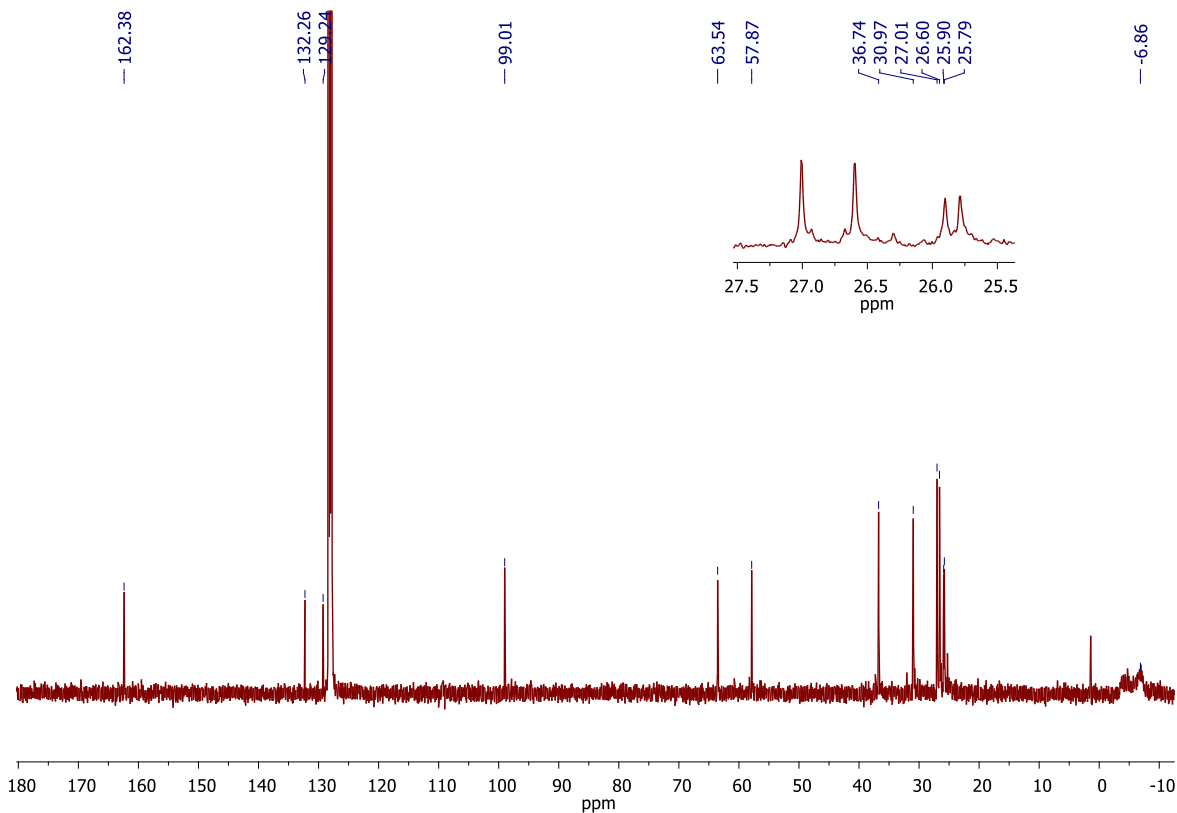


**Figure S9.**  $^{13}\text{C}\{^1\text{H}\}$  NMR spectrum for alkyl aluminum adduct **2** in  $\text{C}_6\text{D}_6$ .

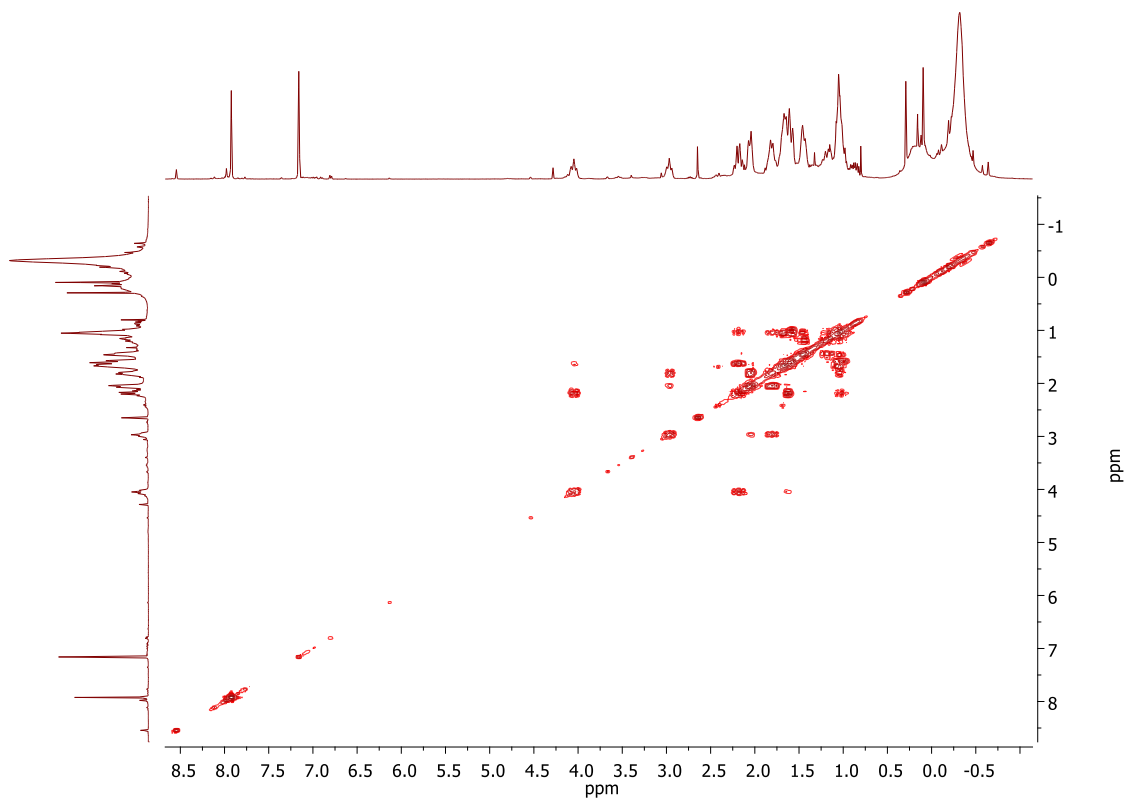


**Figure S10.**  $^1\text{H}$ - $^1\text{H}$  COSY NMR spectrum for alkyl aluminum adduct **2** in  $\text{C}_6\text{D}_6$ .

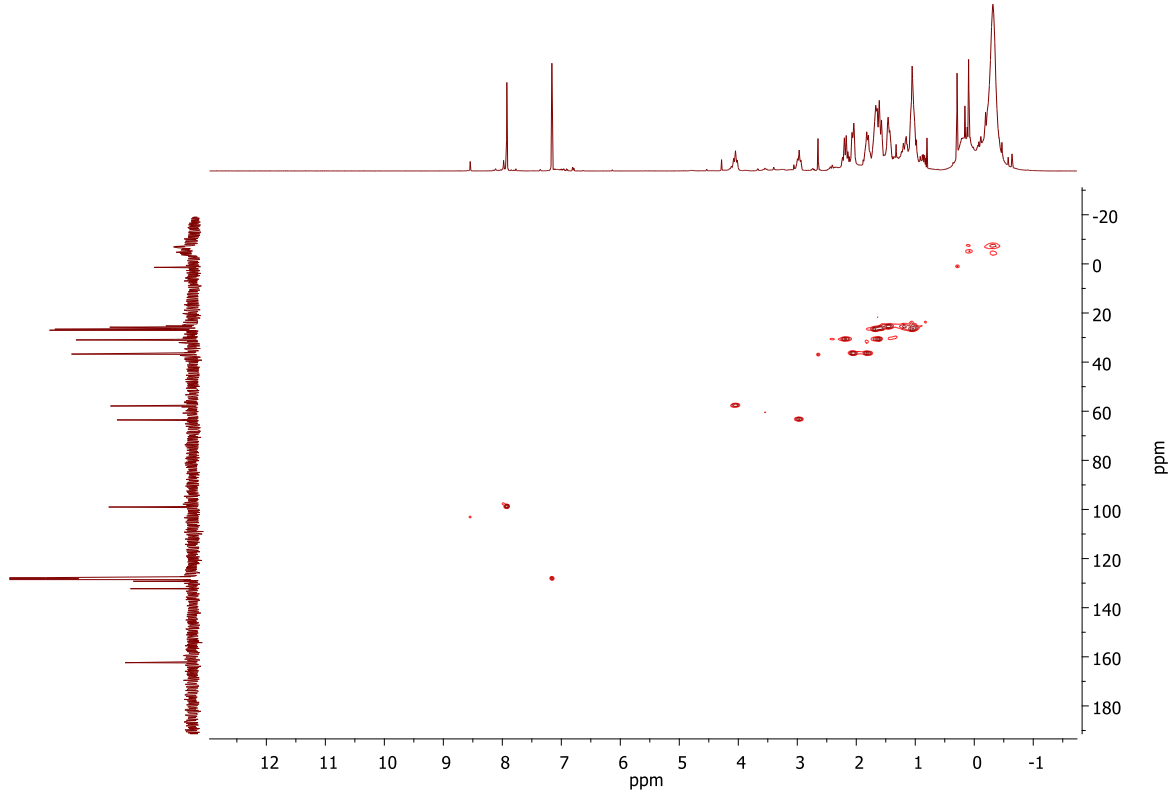


**Figure S11.**  $^{13}\text{C}\{\text{H}\}$ -HMQC NMR spectrum for alkyl aluminum adduct **2** in  $\text{C}_6\text{D}_6$ .

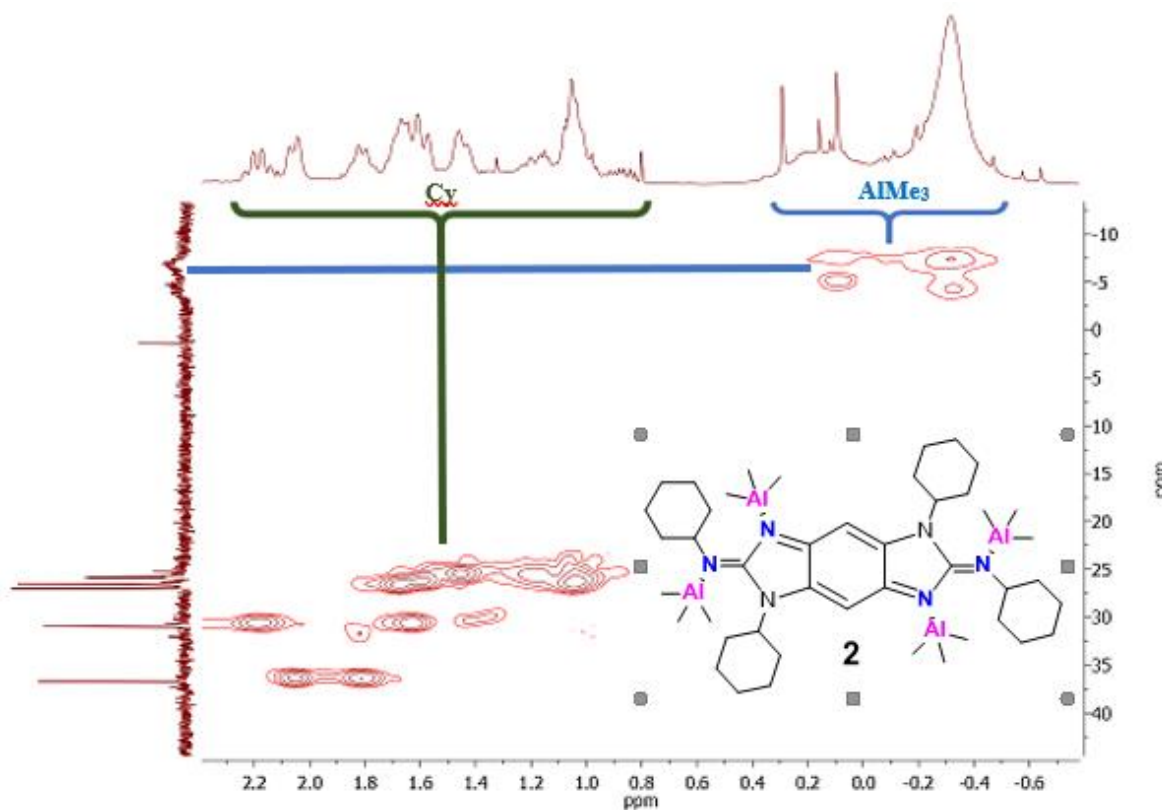


**Figure S12.**  $^{13}\text{C}\{^1\text{H}\}$ -HMQC NMR spectrum for alkyl aluminum adduct **2** in  $\text{C}_6\text{D}_6$  (range  $(-0.8)$ – $2.4$  ppm in  $^1\text{H}$ -NMR and  $(-12.0)$ – $45.0$  ppm in  $^{13}\text{C}$ -NMR).

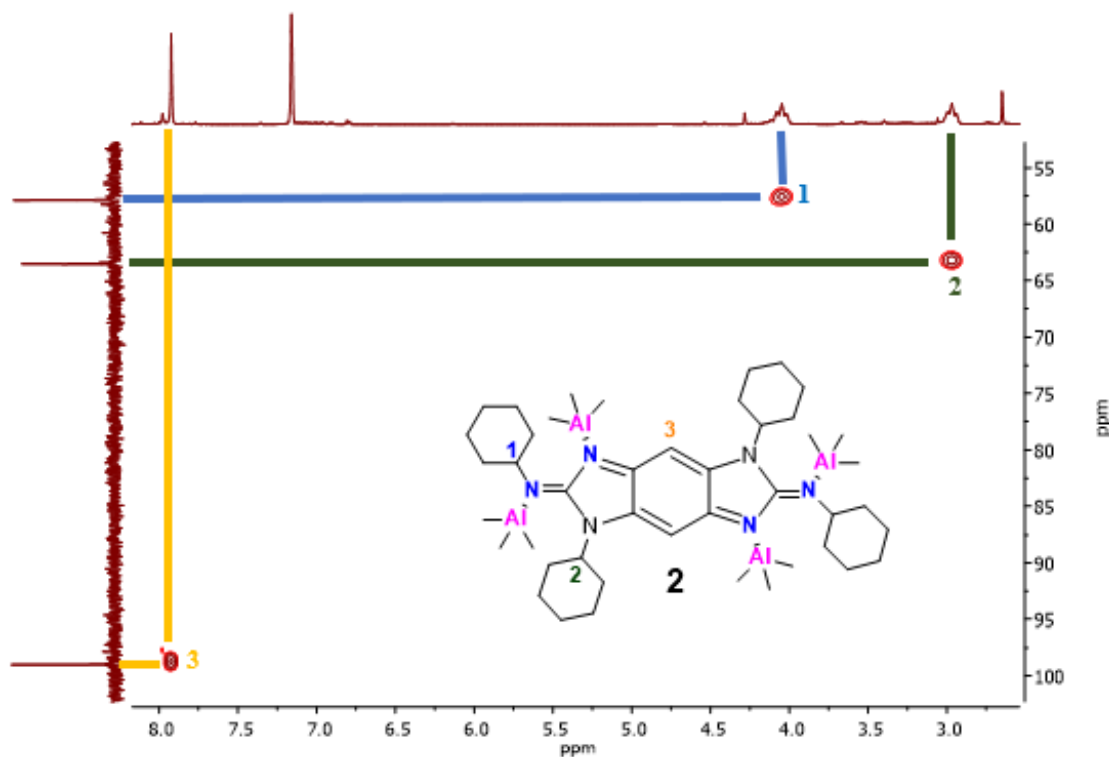


**Figure S13.**  $^{13}\text{C}\{^1\text{H}\}$ -HMQC NMR spectrum for alkyl aluminum adduct **2** in  $\text{C}_6\text{D}_6$  (range  $2.5$ – $8.2$  ppm in  $^1\text{H}$ -NMR and  $53.0$ – $103.0$  ppm in  $^{13}\text{C}$ -NMR).

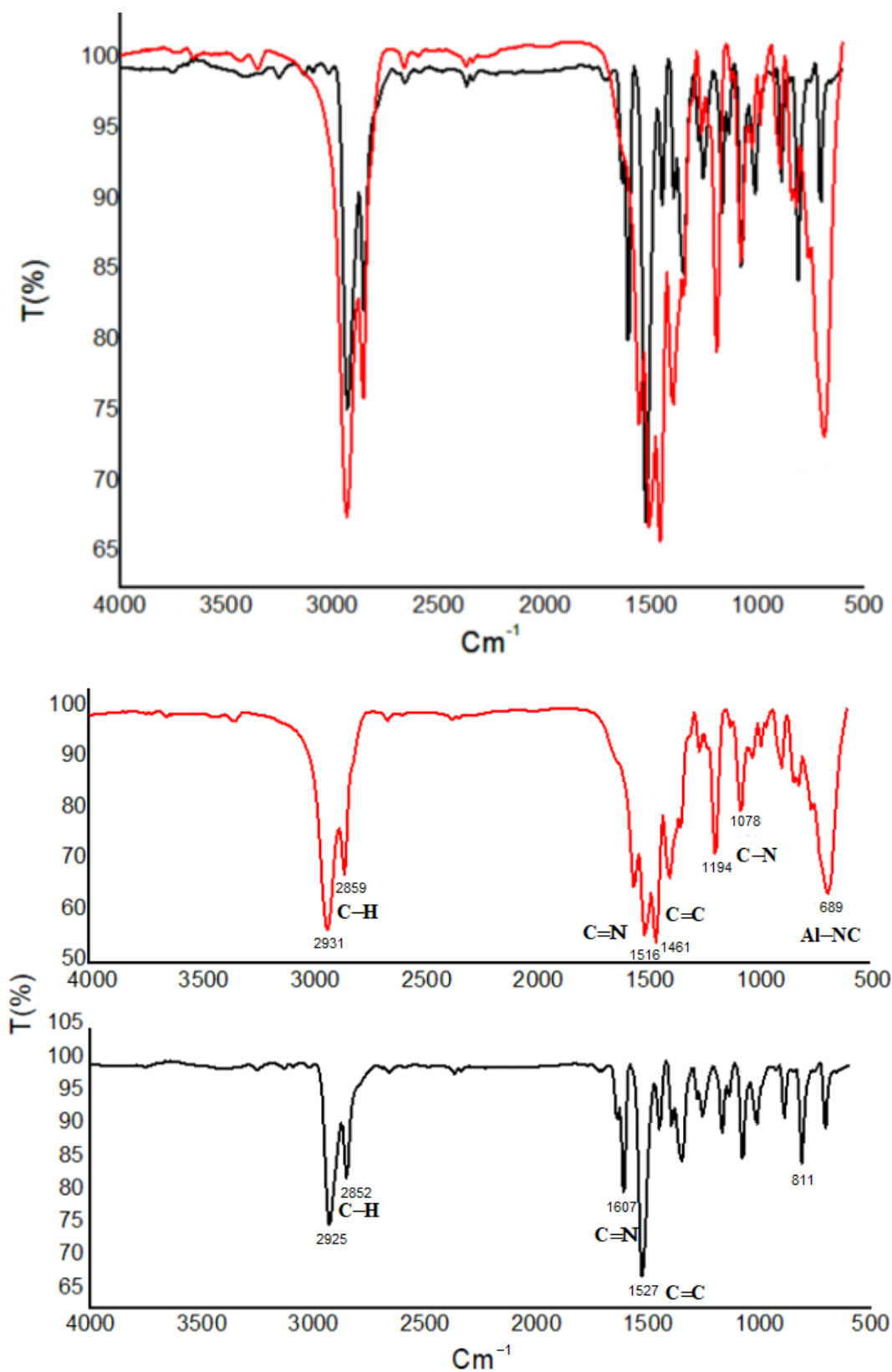


**Figure S14.** FT-IR spectrum for alkyl aluminum adduct 2 (red) versus benzodiimidazole-diylidene ligand L<sub>2</sub> (black).

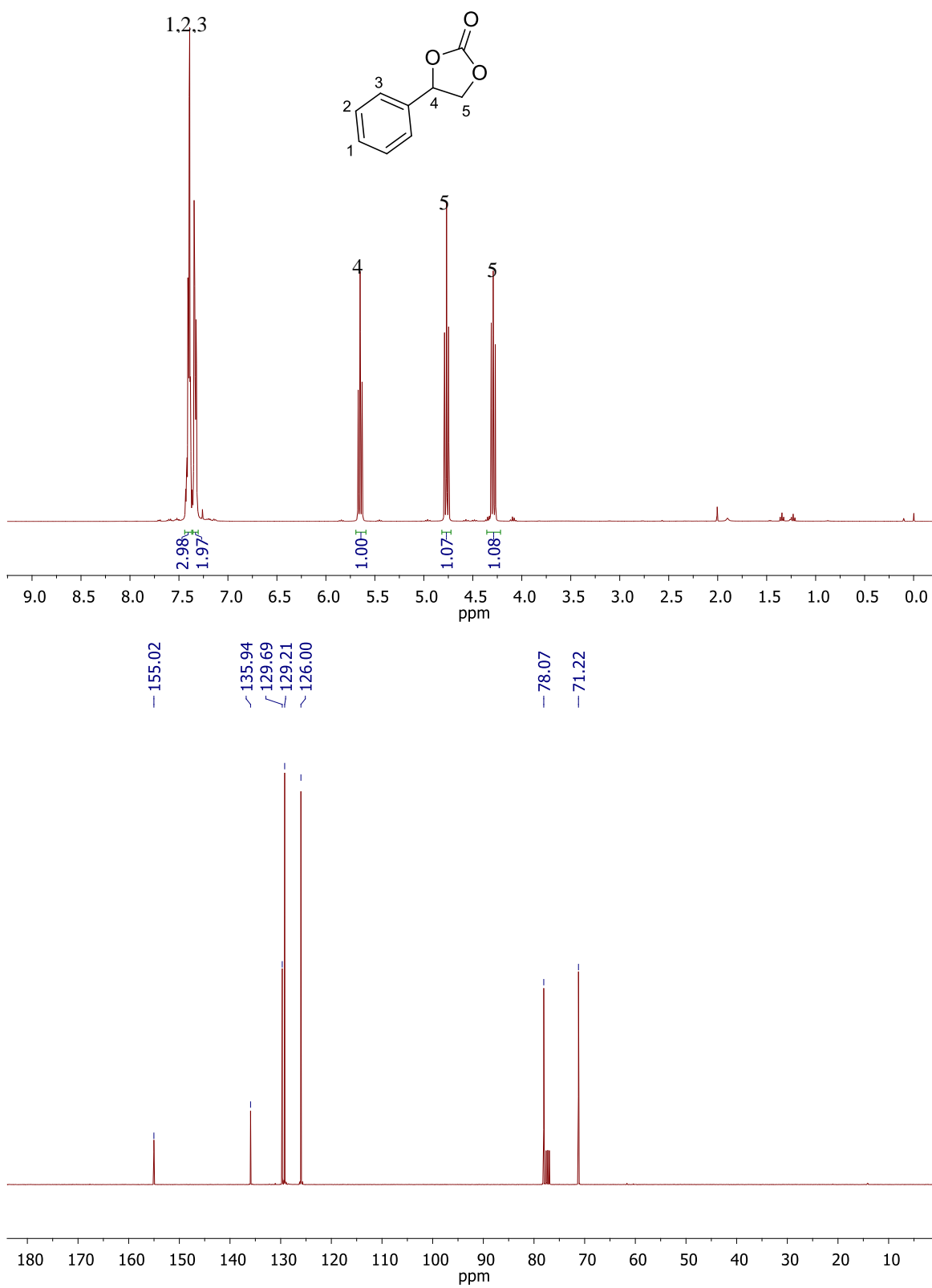
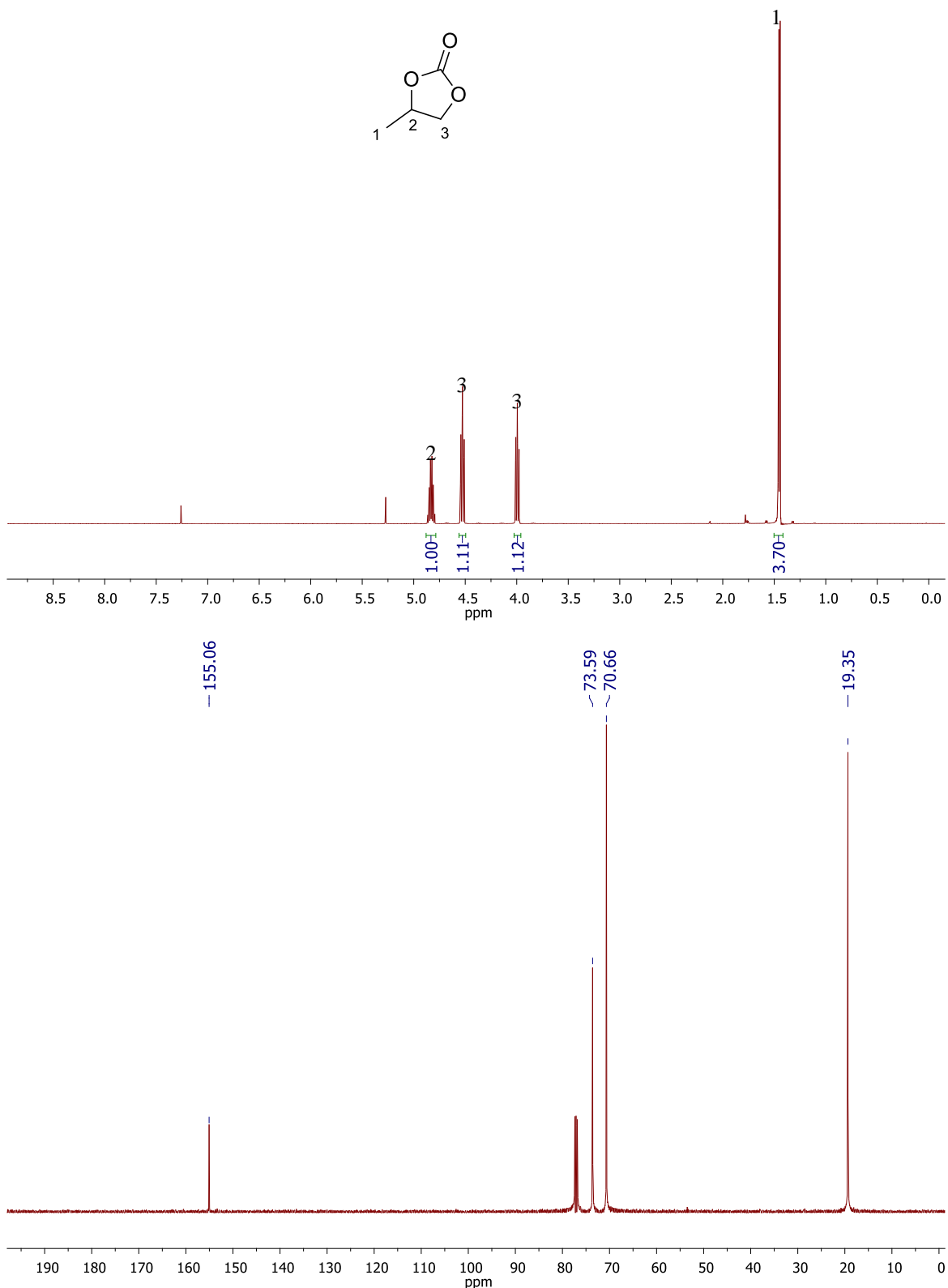
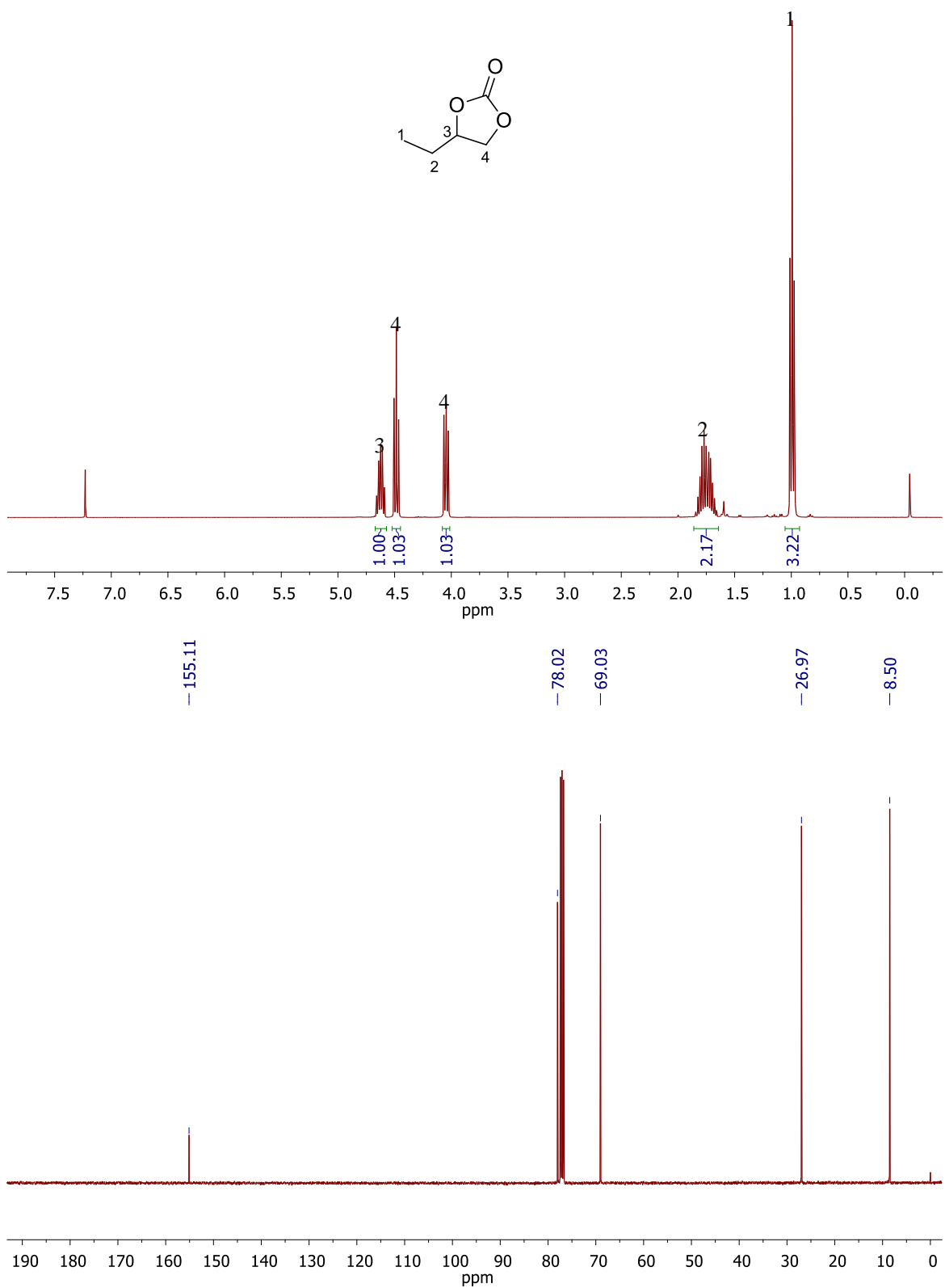


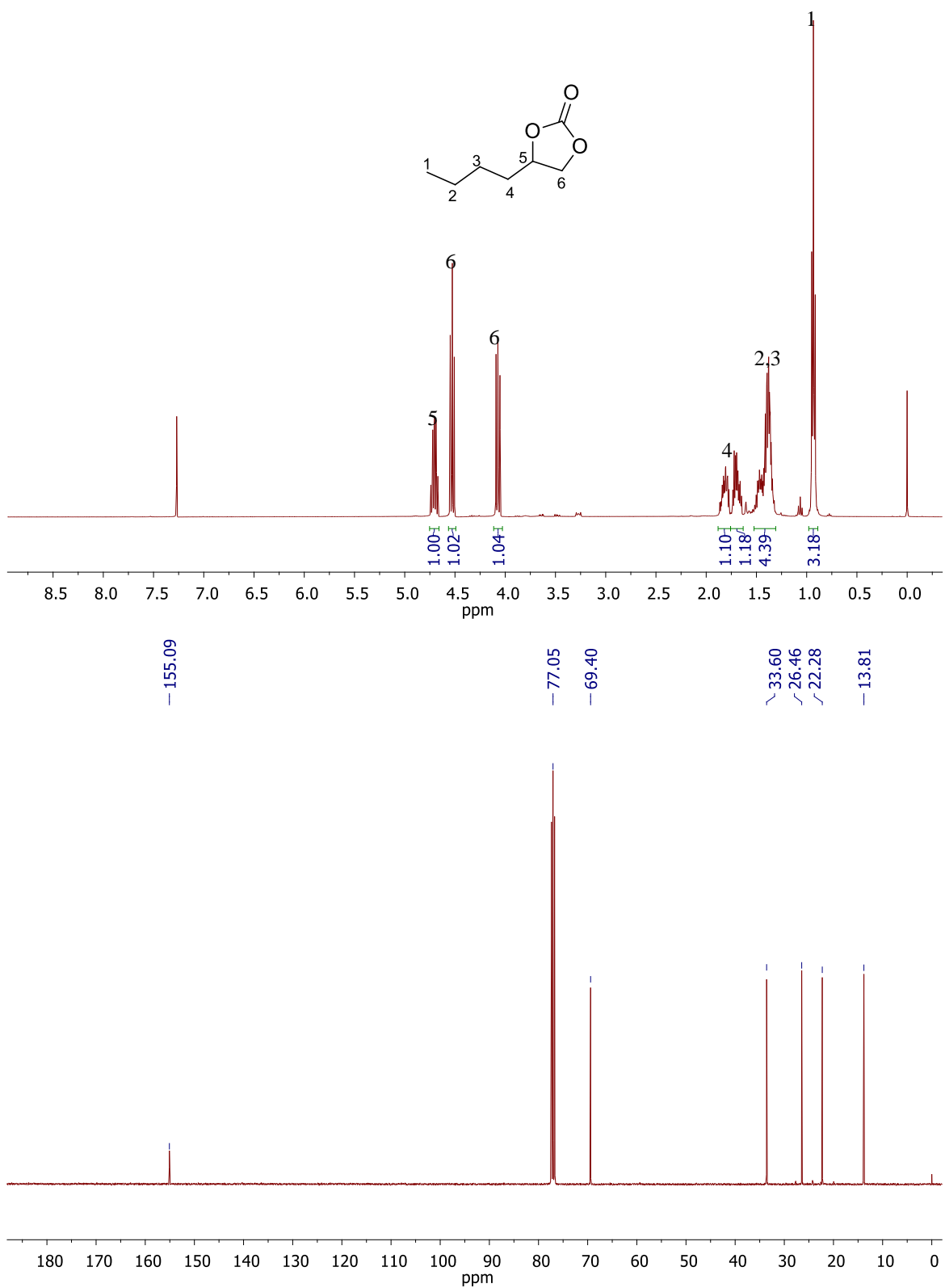
Figure S15. NMR spectra for styrene carbonate **3a** in  $\text{CDCl}_3$ .



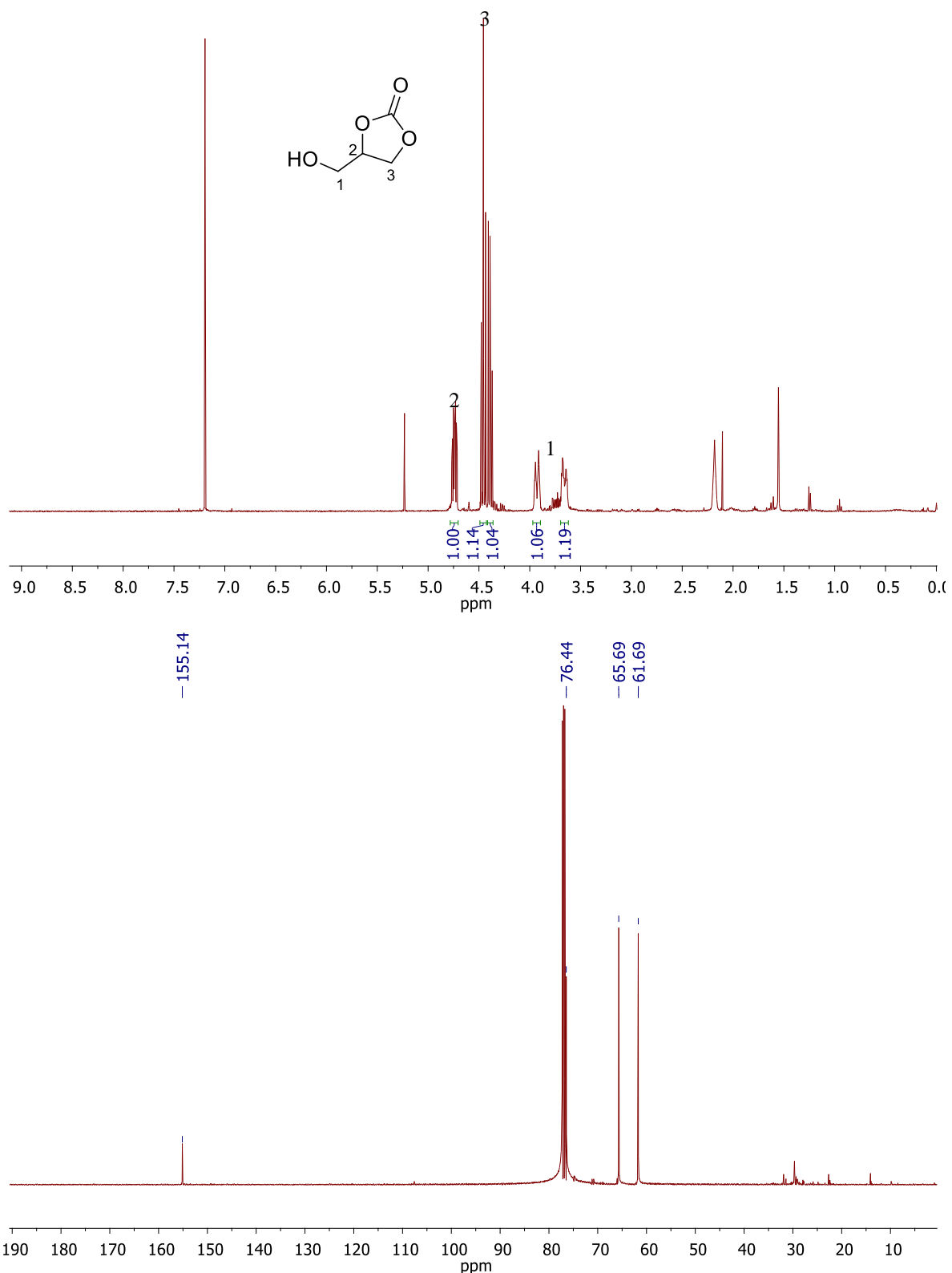
**Figure S16.** NMR spectra for propylene carbonate **3b** in  $\text{CDCl}_3$ .



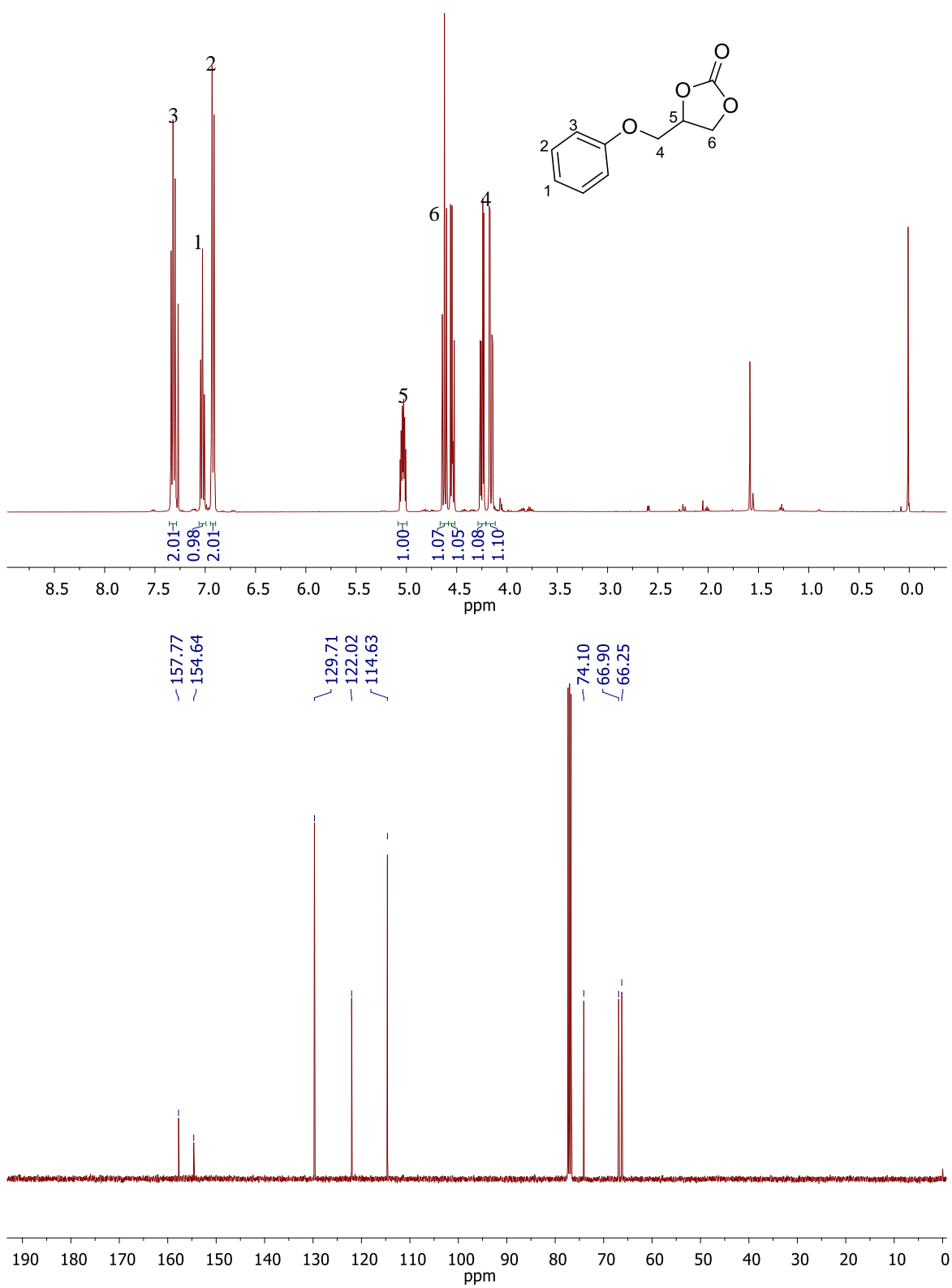
**Figure S17.** NMR spectra for 1,2-butylene carbonate **3c** in  $\text{CDCl}_3$ .



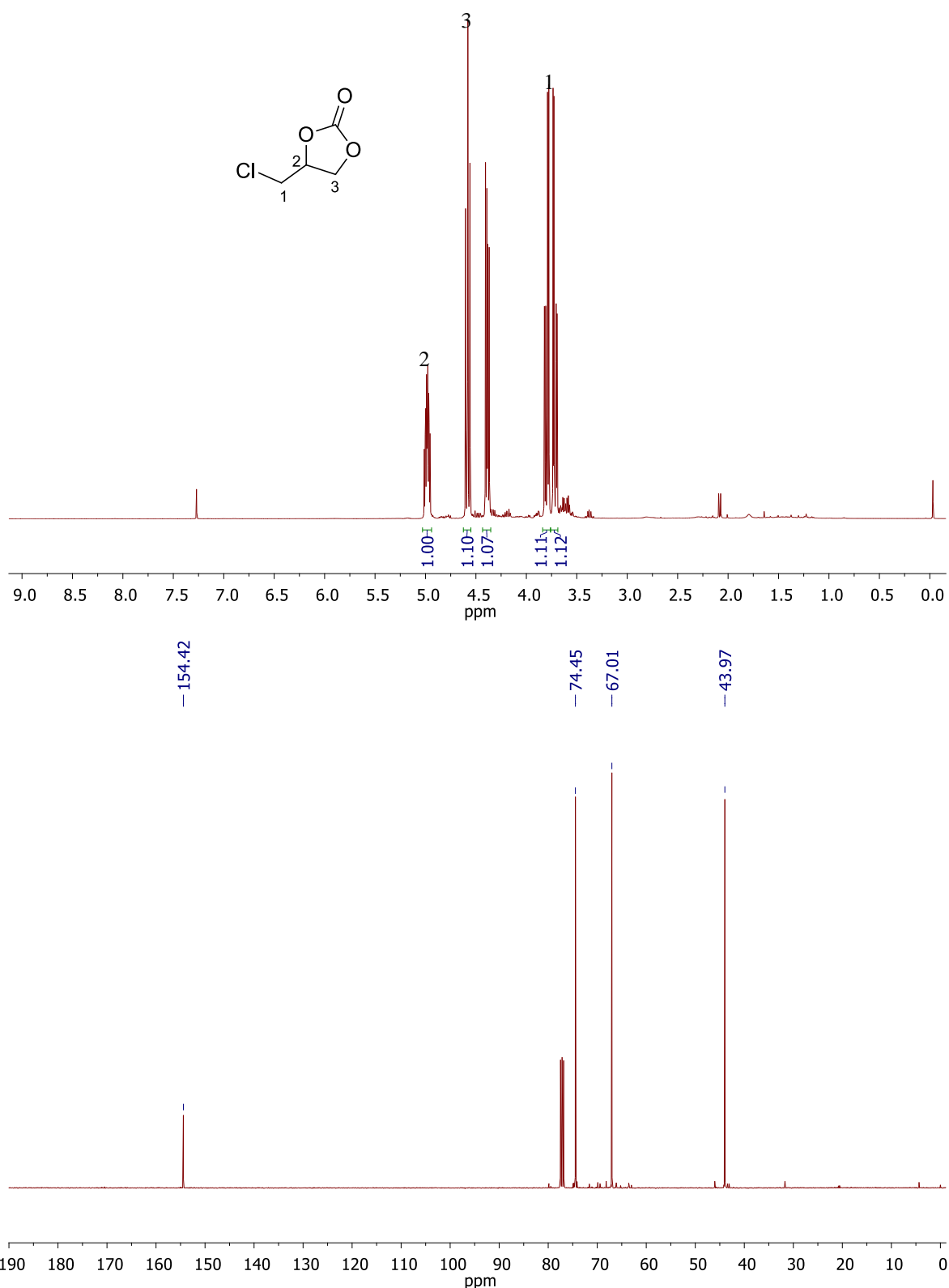
**Figure S18.** NMR spectra for 1,2-hexylene carbonate **3d** in  $\text{CDCl}_3$ .



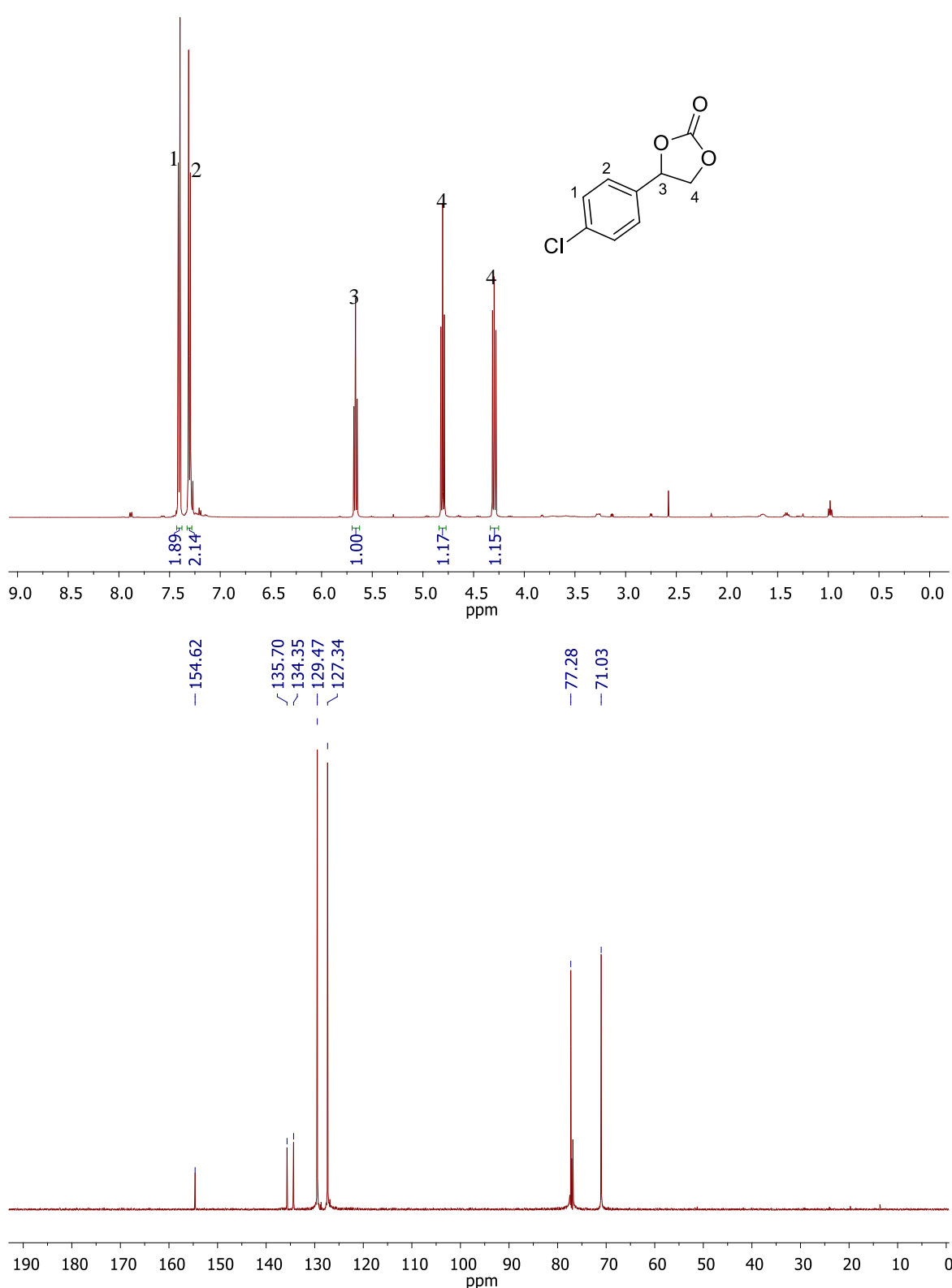
**Figure S19.** NMR spectra for glycerol carbonate **3e** in  $[D_6]DMSO$ .



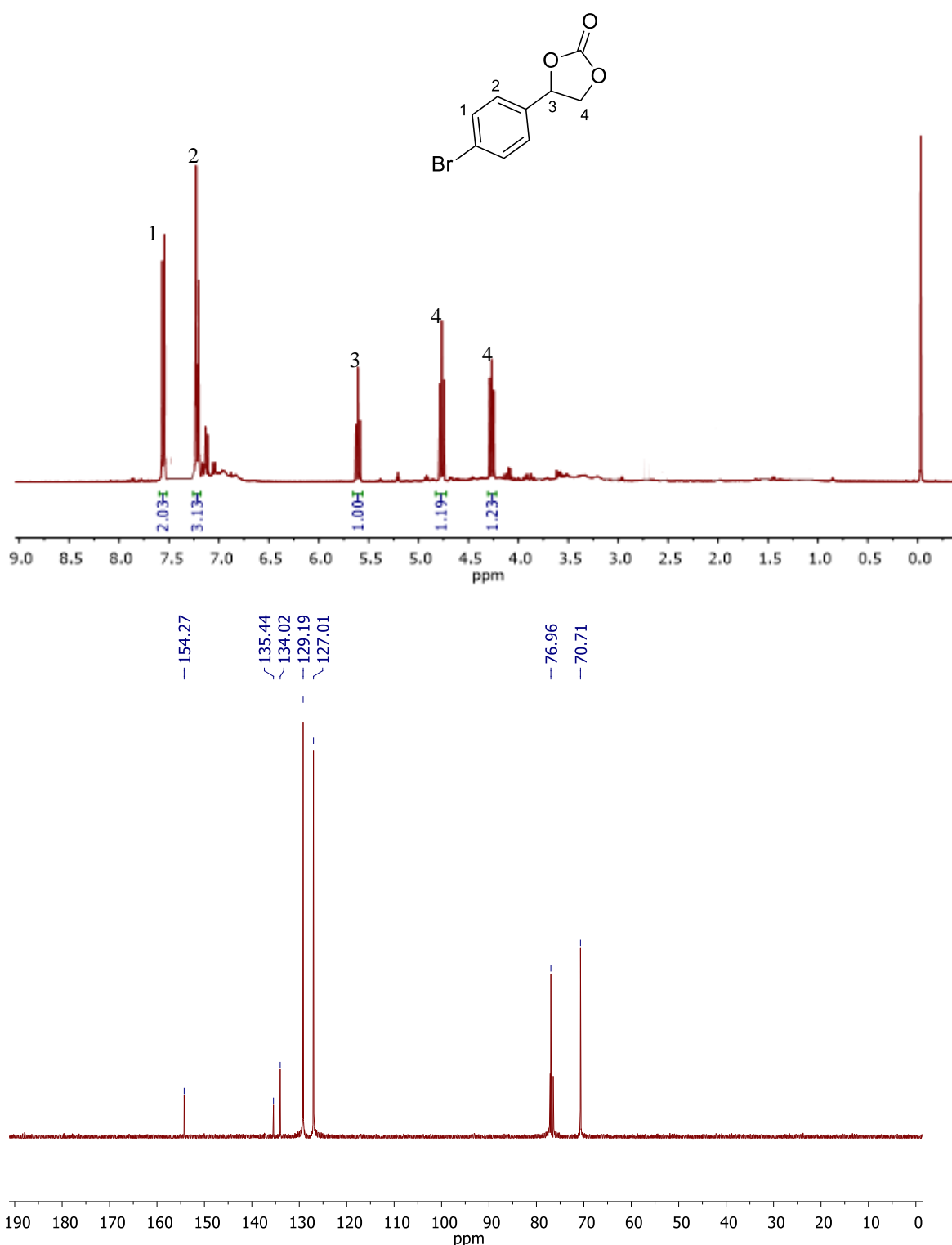
**Figure S20.** NMR spectra for 3-phenoxypropylene carbonate **3f** in  $\text{CDCl}_3$ .



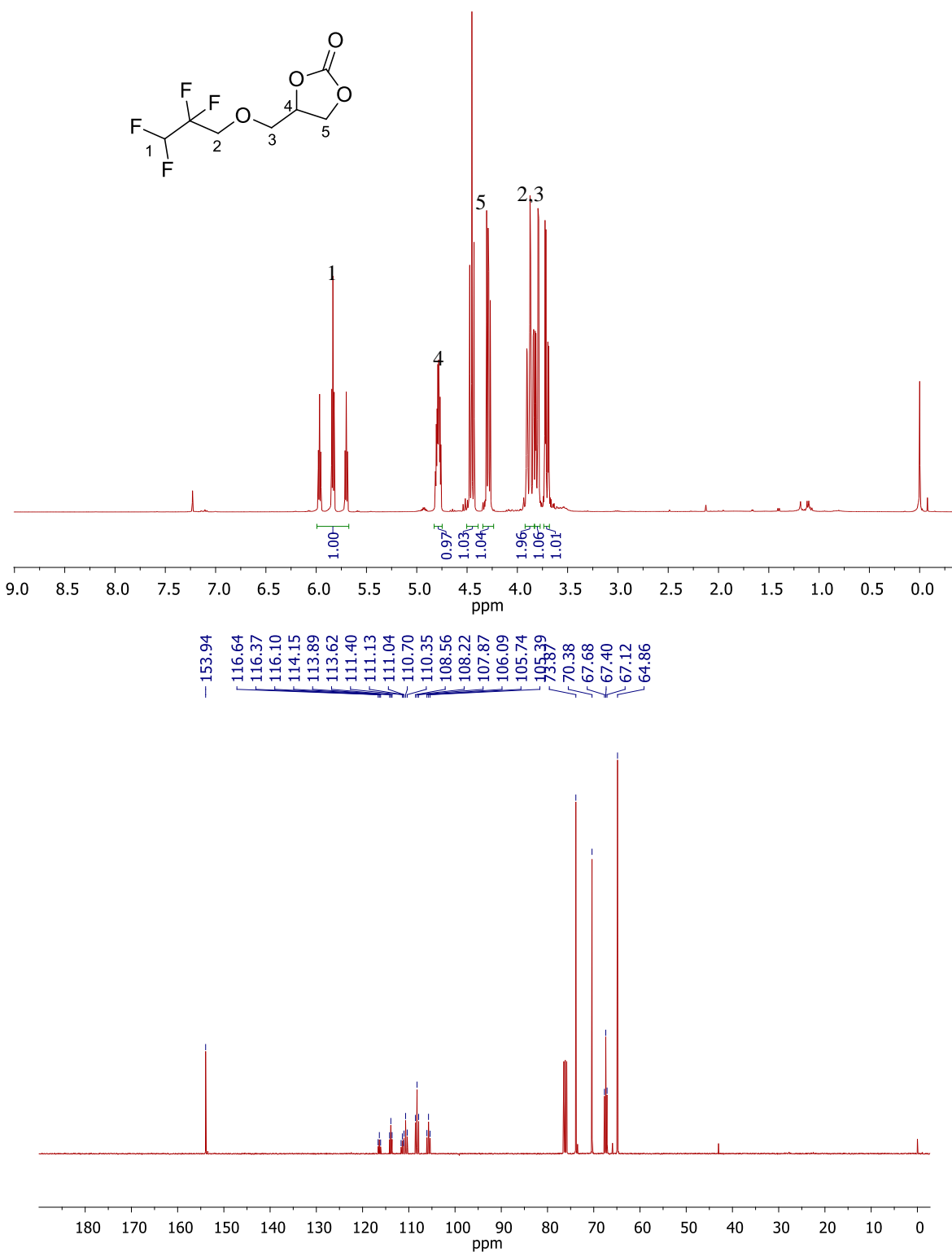
**Figure S21.** NMR spectra for 3-chloropropylene carbonate **3g** in  $\text{CDCl}_3$ .

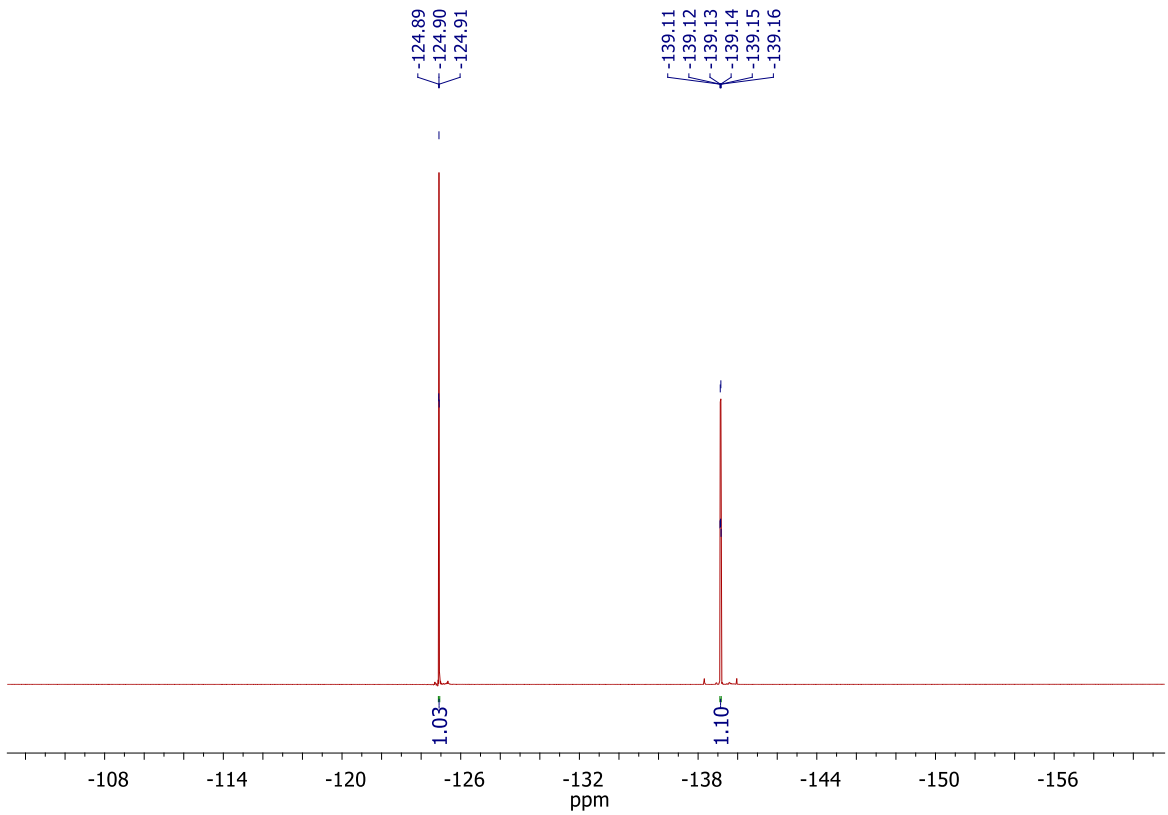


**Figure S22.** NMR spectra for 4-chlorostyrene carbonate **3h** in  $\text{CDCl}_3$ .

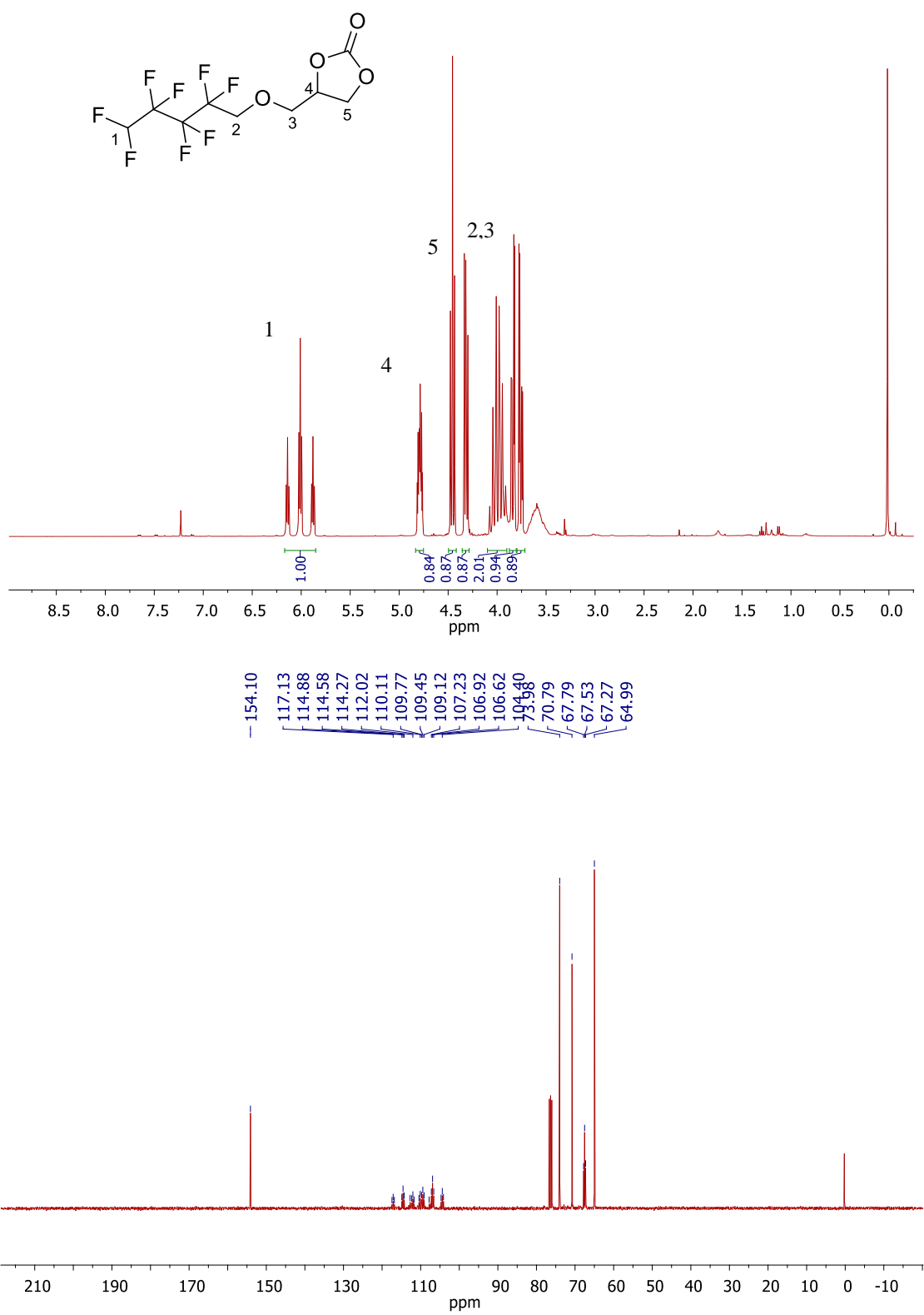


**Figure S23.** NMR spectra for 4-bromostyrene carbonate **3i** in  $\text{CDCl}_3$ .





**Figure 24.** NMR spectra for 4-((2,2,3,3-tetrafluoropropoxy)methyl)-1,3-dioxolan-2-one **3j** in  $\text{CDCl}_3$ .



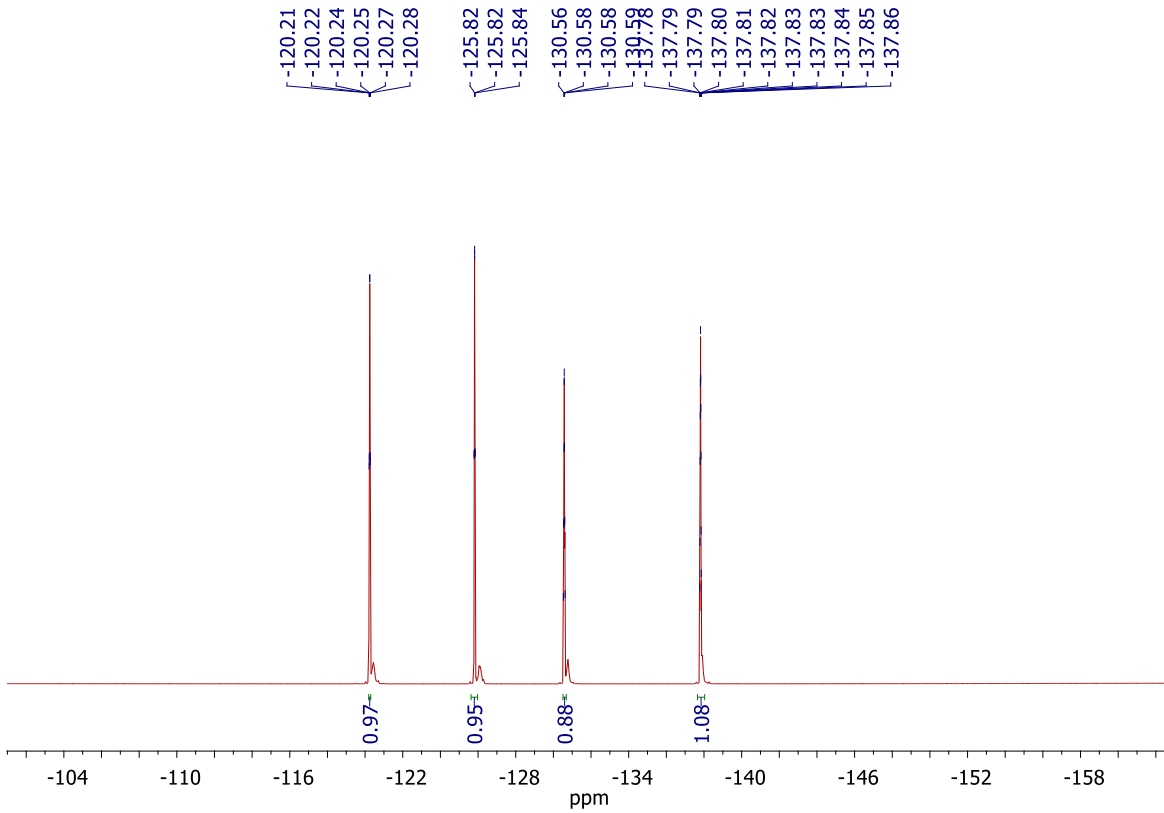


**Figure 25.** NMR spectra for 4-((2,2,3,3,4,4,5,5-Octafluoropentyl)oxy)methyl)-1,3-dioxolan-2-one **3h** in CDCl<sub>3</sub>.

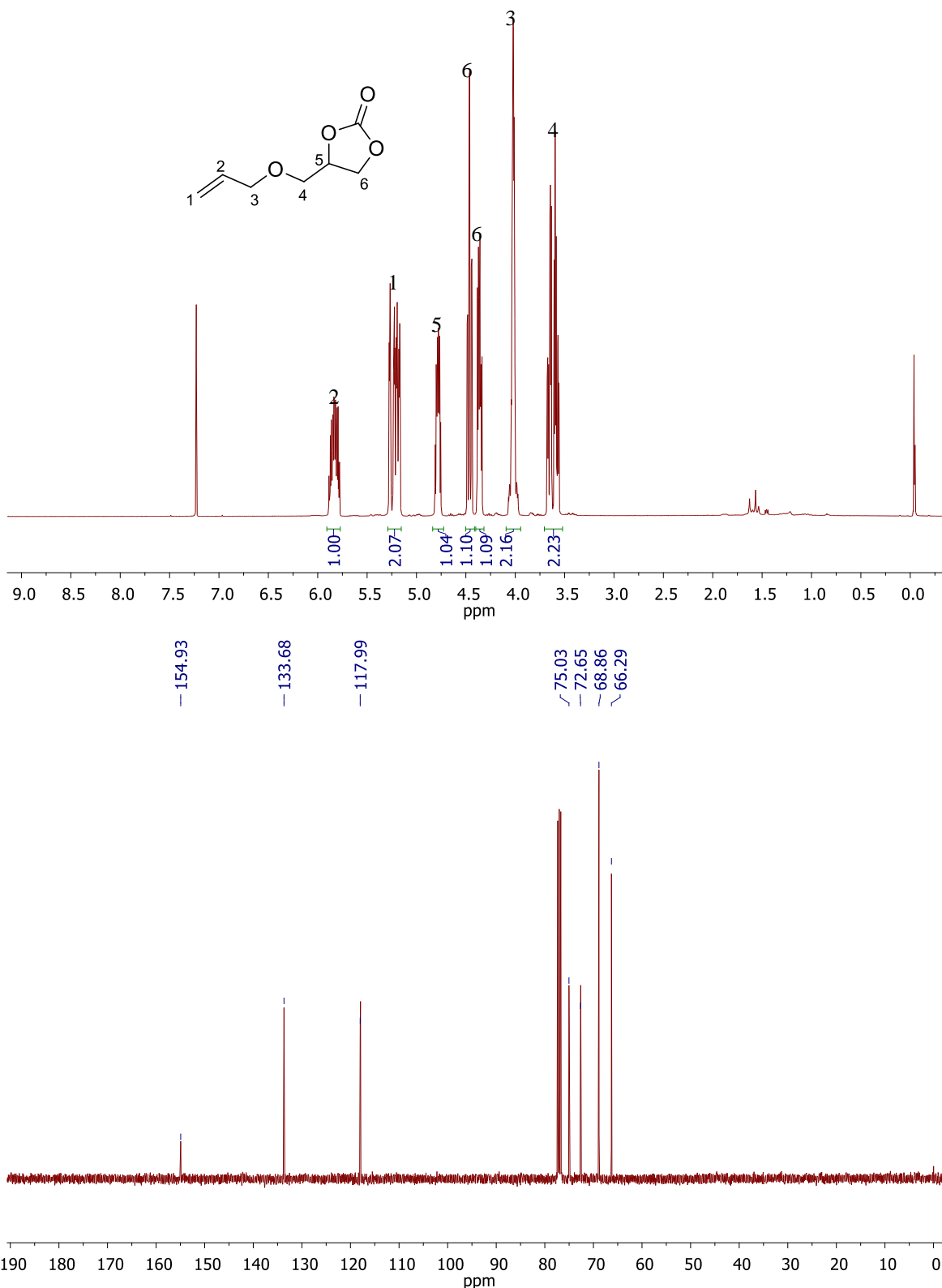


**Figure S26.** NMR spectra for 4-((allyloxy)methyl)-1,3-dioxolan-2-one **3l** in  $\text{CDCl}_3$ .

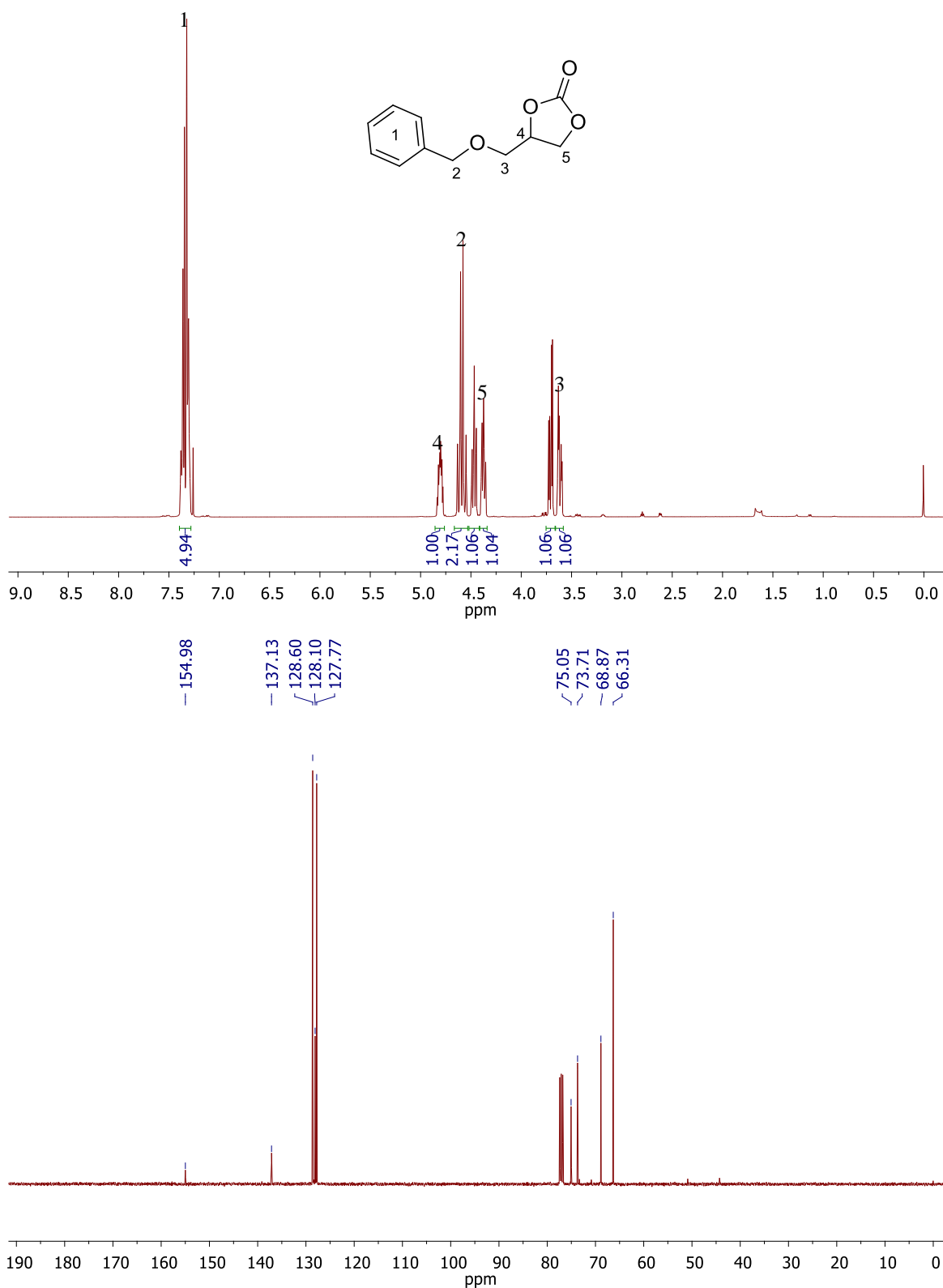


**Figure S27.** NMR spectra for 4-((benzyloxy)methyl)-1,3-dioxolan-2-one **3m** in CDCl<sub>3</sub>.

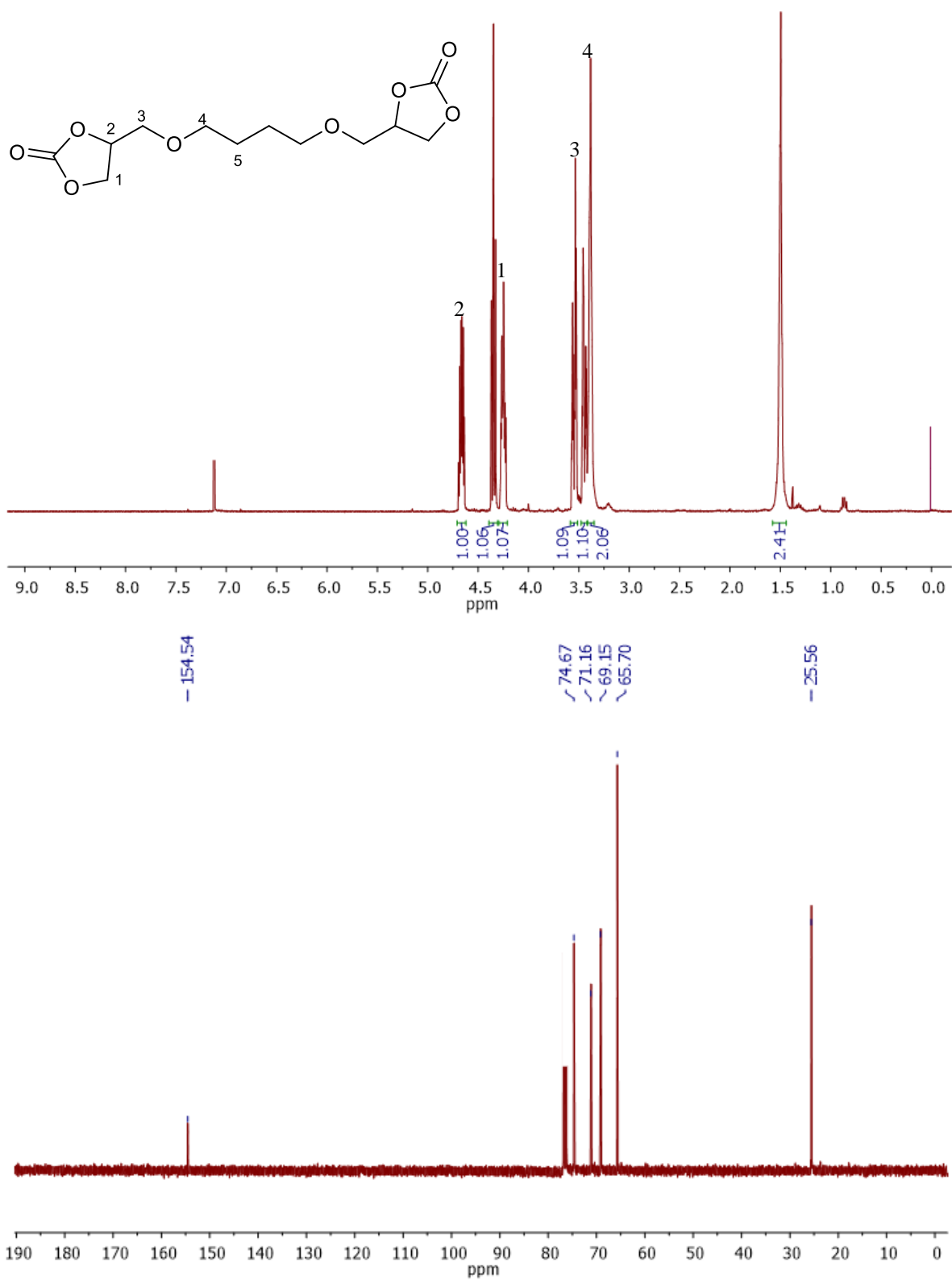


**Figure S28.** NMR spectra for 4,4'-(butane-1,4-diylbis(oxy))bis(methylene)bis(1,3-dioxolan-2-one) **3n** in CDCl<sub>3</sub>.

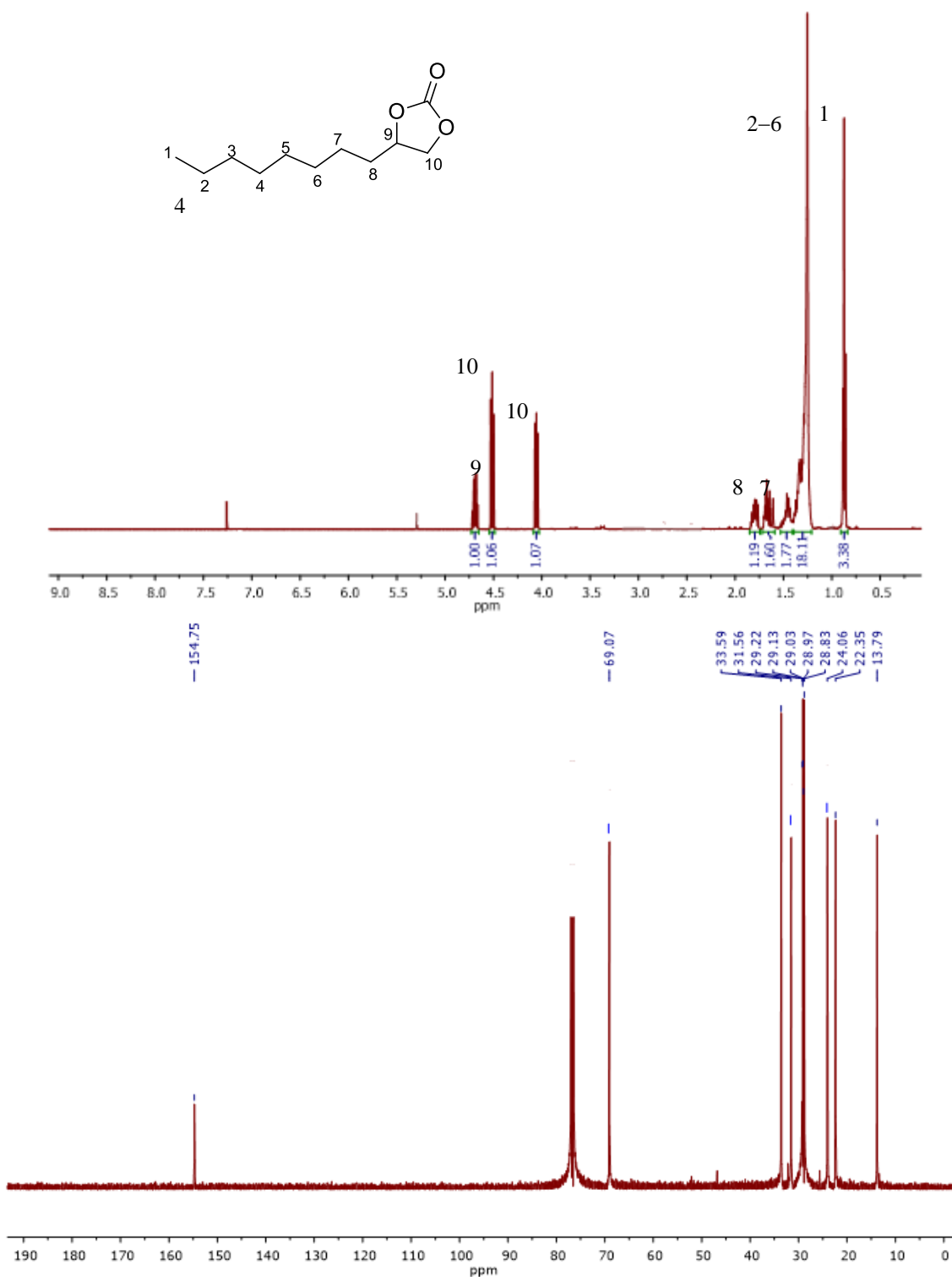


**Figure S29.** NMR spectra 1,2-Decylene carbonate **3o** in  $\text{CDCl}_3$ .

**Publisher's Note:** MDPI stays neutral with regard to jurisdictional claims in published maps and institutional affiliations.



© 2020 by the authors. Submitted for possible open access publication under the terms and conditions of the Creative Commons Attribution (CC BY) license (<http://creativecommons.org/licenses/by/4.0/>).